Final Draft
of the original manuscript:

Lemmen, C.; Wirtz, K.W.:
On the sensitivity of the simulated European Neolithic transition to climate extremes
In: Journal of Archaeological Science (2012) Elsevier

DOI: 10.1016/j.jas.2012.10.023

On the sensitivity of the simulated European Neolithic transition to climate extremes

Carsten Lemmen*, Kai W. Wirtz

Helmholtz-Zentrum Geesthacht, Institute of Coastal Research, Max-Planck Straße 1, 21501 Geesthacht, Germany

Abstract

Was the spread of agropastoralism from the Fertile Crescent throughout Europe influenced by extreme climate events, or was it independent of climate? We here generate idealized climate events using palaeoclimate records. In a mathematical model of regional sociocultural development, these events disturb the subsistence base of simulated forager and farmer societies. We evaluate the regional simulated transition timings and durations against a published large set of radiocarbon dates for western Eurasia; the model is able to realistically hindcast much of the inhomogeneous space-time evolution of regional Neolithic transitions. Our study shows that the consideration of climate events improves the simulation of typical lags between cultural complexes, but that the overall difference to a model without climate events is not significant. Climate events may not have been as important for early sociocultural dynamics as endogenous factors.

Key words: Europe, climate events, extreme events, Neolithic transition, adaptation, modeling

1. Introduction

Between 10 000 and 3000 cal BC, western Eurasia saw enormous cultural, technological, and sociopolitical changes with the emergence of agropastoralism, permanent settlements, and state formation (Barker, 2006). Human population experienced a dramatic increase (Bocquet-Appel, 2008; Gignoux et al., 2011), and people, plants and animals moved or were moved great distances (e.g., Zohary and Hopf, 1993).

While the Holocene possibly defines the start of major anthropogenic global environmental change (Lemmen, 2010; Kaplan et al., 2011), it also marks the period where climatic shifts could have affected human subsistence more severely than ever before: reduced mobility after investments in settlement infrastructure most likely increased the sensitivity of the novel farmers to environmental alterations (Janssen and Scheffer, 2004). There remains, however, considerable uncertainty on whether and how climate instabilities had influenced the development and spread of agropastoralism in Eurasia (Berglund, 2003; Coombes and Barber, 2005).

1.1. Origin and spread of western Eurasian farming

The Neolithic originated most probably in the Fertile Crescent, between the Levantine coast and the Zagros ridge. In this region, almost all European food crops and animals—wheat, barley, cattle, sheep, pigs—had been domesticated and inserted into a broad spectrum of foraging practices during the tenth millennium cal BC (Flannery, 1973; Zeder, 2008). Neolithic (farming based) life style emerged not before the 9th millennium BC in this core region (Rosen and Rivera-Collazo, 2012), and expanded to Cyprus by 8500 cal BC (Peltenburg et al., 2000); around 7000 cal BC, agropastoralism appeared on the Balkan and in Greece (Perlès, 2001). Propagating in a generally northwestern direction, agropastoralism finally arrived after 4000 cal BC on the British isles and throughout northern Europe (Sheridan, 2007); in a western direction, the expansion proceeded fast along the Mediterranean coast to reach the Iberian peninsula at 5600 cal BC (Zapata et al., 2004).

1.2. Transitions and climate

It has been argued that a precondition of agriculture was the relatively stable environment of the Holocene (Feynman and Ruzmaikin, 2007), and that only in this stable environment active cultivation and establishment of infrastructure such as fields and villages was favored (van der Leeuw, 2008). Within its relative stability, however, the Holocene climate exhibited variability on many spatial and temporal scales with pronounced multi-centennial and millennial cycles (Mayewski et al., 2004; Wanner et al., 2008). In addition, non-cyclic anomalies have been identified (e.g., Wirtz et al., 2010), most prominently the so-called 8.2 and 4.2 events (around 6200 and 2200 cal BC, respectively, von Grafenstein et al. 1998; Cullen et al. 2000). Although the regional scale and intensity of the 4.2 event has been strongly questioned (e.g., Finné et al., 2011), the event had evoked the formulation of hypotheses on the connection between climatic disruptions and societal collapse (Weiss

*Tel +49 4152 87-2013, Fax -2020

Email address: carsten.lemmen@hzg.de (Carsten Lemmen)

et al., 1993; DeMenocal, 2001). Similarly, the globally documented 8.2 event has been linked to the abandonment of many settlements in the Near East and simultaneous appearance of new village structures in southeast Europe (Weninger et al., 2005).

It might be coincidental that the 8.2 and 4.2 events define the time window of the Neolithic expansion in Europe, but the general view that environmental pressure on early Neolithic populations may have stimulated outmigration has been put forward since long (Childe, 1942). Dolukhanov (1973), Gronenborn (2009, 2010), or Weninger et al. (2009) suggest that climate-induced crises may have forced early farming communities to fission and move in order to escape conflicts. Berger and Guilaine (2009), to the contrary, see the role of climate events rather in creating opportunities: the rapid farming expansion into the Balkan could have been stimulated by an increase of natural fires after the 8.2 event, which opened up the formerly forested landscape.

1.3. How sensitive was the Neolithization to climate?

The relevance of climate variability and external triggers for prehistoric agricultural dynamics has been severely questioned (e.g., Erickson, 1999; Coombes and Barber, 2005). Alternative theories of the Neolithic transition underline the agency of early societies (Shanks and Tilley, 1987; Whittle and Cummings, 2007). On the other hand, the development of technological, social, and cultural complexes can hardly be thought to evolve independently of their variable environments; and the spatio-temporal imprint of the Neolithization in Eurasia requires a geographic approach which resolves how people and/or goods and practices migrated over long distances. Berglund (2003), e.g., suggested a stepwise interaction between agriculture and climate but found no strong links for northwest Europe.

The dispersal of agriculture into Europe has long been mathematically formulated based on Childe's (1925) observation on the spatiotemporal distribution gradient of ceramics that Ammerman and Cavalli-Sforza (1971) formulated as the 'wave of advance' model. This simple—and also the later more advanced ones (Ackland et al., 2007; Galeta et al., 2011; Davison et al., 2006)—diffusion models received support from linguistic (e.g. Renfrew, 1987) and archaeogenetic work (e.g. Balaresque et al., 2010). The dispersal of agriculture in these models occurs concentrically, and can be modulated by topography and geography. This dispersal model is not able to describe the inhomogeneous spatiotemporal distribution of radiocarbon dates, which are, e.g., apparent in regionally different stagnation periods ('hypothèse arythmique', Guilaine, 2003; Rasse, 2008; Schier, 2009).

Stagnations are visible in the simulation by Lemmen et al. (2011), who integrate endogenous regional sociocultural dynamics with the dispersal of agriculture. Their approach connects social dynamics—as optimally evolving agents—to regionally and temporally changing environments; in addition, they account for the spatio-temporal spread of populations and technological traits. Their Global Land Use and technological Evolution Simulator (GLUES) has proven to produce realistic hindcasts of the origin and distribution of agropastoralism and concomitant cultures around the globe (Wirtz and Lemmen, 2003; de Vries et al., 2002), for Eastern North America (Lemmen, 2012), the Indus valley (Lemmen and Khan, 2012), and western Eurasia (Lemmen et al., 2011). Using GLUES and a globally synchronous climate forcing signal, Wirtz and Lemmen (2003) found a general delay of the simulated regional Neolithic due to climate fluctuations; at a global scale, differences in hindcasted socio-cultural trajectories proved to be largely independent of temporal disruptions.

We here use temporal disruptions that are defined as excursions of a climate variable far from the local mean climate, i.e. extreme climate events; we do not consider rapid climate shifts that abruptly alter the climate mean state (e.g., Dakos and Scheffer, 2008). The hypothesis that extreme climate events had significant impacts on the Neolithization of Europe is critically examined: we employ GLUES as a deductive tool to reconstruct the Neolithic transition in Europe and evaluate the simulated reconstruction against the radiocarbon record of Neolithic sites in two experiments: (1) one including climate events, represented by a pseudo-realistic spatially resolved climate event history for the period 9500–3000 cal BC; and (2) another without climate events.

2. Material and Methods

2.1. Reconstructing climate event history

We used a data collection of 134 globally distributed, high-resolution (< 200 a) and long-term (> 4000 a) palaeoclimate time series collected from public archives and published literature. The collection only contains studies where the respective authors indicated a direct relation to climate variables such a precipitation, temperature, or wind regime (e.g. Bond, 1997; Wick et al., 2003; Chapman and Shackleton, 2000; Gasse, 2000). A large part of this data set (122 time series) was previously analyzed by Wirtz et al. (2010) for extreme events; a complete overview of time series in this collection is provided in the supporting online material (Table S1). Due to the different types of proxies originating from both marine and terrestrial sites (mostly δ^{18}O, see Table 1) the relation to climate variables is often ambiguous, also in sign. This ambiguity does not affect our analysis, as we are only interested in the spatio-temporal characterization of extreme events: a drastic excursion from a climate mean state stressed regional habitats and human populations regardless of its direction.

Our data set comprises 134 palaeoclimate time series, all of them long-term and high-resolution, and provides the best spatial and temporal coverage of any study we are aware of. Previous collections used 18, 50, 60 or 80 records (Wanner et al. 2008; Mayewski et al. 2004; Holmgren et al.

2003; Finné et al. 2011, respectively), mostly limited to the last 6000 years. The coverage we use here is sufficient to represent climate variability in almost all land areas of the world (with sparsest regional coverage in central Australia, Saharan Africa, and Northern-Central Eurasia), considering the spatial coherence of climate signals within 1500 km distance found by Wirtz et al. (2010) for their similar data set.

From the global dataset, 26 time series are located in or near our focus area western Eurasia (Table 1). For these time series we analyzed the non-cyclic event frequency according to the procedure in Wirtz et al. (2010): time series were detrended with a moving window of 2000 years and smoothed with a moving window of 50 years, then normalized (Figure 1b). Events were detected whenever a time series signal exceeded a confidence interval with threshold $p = 1 - 1/n$, where n is the number of data points (Thomson, 1990), and where each event is preceded or followed by a sign change in the time series.

For each simulation region, events from spatially overlapping or nearby proxy locations were used to construct an aggregated event time series specific to this region (Figure 1a–c): (1) a Gaussian filter with $\tau = 175$ a (corresponding to the dating uncertainty in many records) standard deviation was applied to each event; (2) the distance of the proxy location to the simulation region was used to assign exponentially decreasing weights to each event; (3) all event densities were summed and filtered with a running mean with window τ; (4) all events representing single anomalies above the mean event density were used for further analysis, irrespective of their magnitude. On average, seven events were detected per time series.

From this analysis, we obtain a pseudo-realistic data base of spatially and temporally resolved climate events. By using this idealized approach, we show a way to overcome issues raised by, e.g., Schulting (2010) on chronological resolution and spatial representation problems of individual records. In our study, we consider the impact of the number of extreme events and their spatial patterning rather than single chronologies. This idealized—or potential—climate events database thus allows us to go forward with analyzing the climate-human relationship while the reliability of individual palaeoclimate reconstructions is still being questioned.

2.2. Global Land Use and technological Evolution Simulator

The Global Land Use and technological Evolution Simulator (GLUES, Wirtz and Lemmen 2003; Lemmen 2010; Lemmen et al. 2011) was developed to study how differences in cultural trajectories at the region scale can be attributed to the specific adaptation of local societies. GLUES mathematically resolves the dynamics of local human populations' density and characteristic sociocultural traits in the context of a changing biogeographical environment. One of the characteristic traits represents available

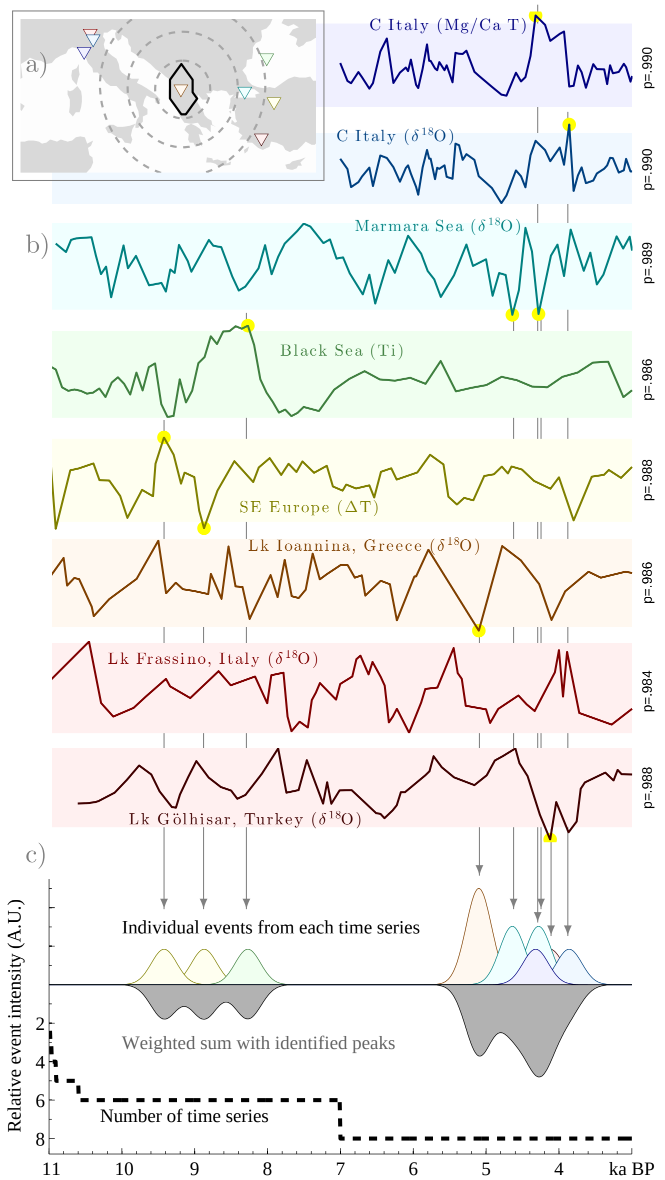

Figure 1: Generation of idealized climate events. (a, top) Map with example region and nearby locations (colored triangles) where long-term and high-resolution palaeoclimate information is available; concentric circles indicate the distance from the simulation region. (b) Associated palaeoclimate time series, detrended and normalized; for each time series, the confidence level p is indicated and visualized as the width of the background shading. Climate extremes are identified outside this confidence interval and are highlighted. (c, bottom) Contribution of individual extreme events from palaeoclimate time series (weighted by distance and color-coded as above) to the probability distribution of event occurrence in the simulation region. The dotted line shows the number of time series contributing to the event generation for this region.

technologies, a second one the share of farming and herding activities, and the third one the number of established agropastoral economies. Trait characteristics adapt according to a growth-benefit gradient dynamics (e.g. Smith et al., 2011, for ecological applications). Traits are further exchanged between simulation regions by information dis-

Table 1: Table of 26 palaeoclimate time series and associated timing of extreme climate events. This is a subset (relevant for the Western Eurasian focus area) of the entire global collection used to generated extreme climate events; the full dataset is shown in the supplementary material Table S1. Abbreviations: Lk=Lake, Cv=Cave, SST=sea surface temperature, T=temperature, T7=July temperature, P=precipitation, GSD=grayscale density, Ti=Titanium content, and HSG=hematite stained glass.

No	Site	Proxy	Events (cal BC)	Reference	No	Site	Proxy	Events (cal BC)	Reference
49	Trop Atlantic	SST	none	DeMenocal et al. 2000	68	N Finland	T	6940/5160	Husum and Hald 2004
50	N Atlantic	HSG	4100	Bond et al. 2001	69	N Atlantic	GSD	9380/9300 8090/3790	Chapman and Shackleton 2000
52	Ireland	δ^{18}O	8960/8140	McDermott 2004	70	Marmara Sea	δ^{18}O	3590/3230	Sperling et al. 2003
53	NW Morocco	δ^{18}O	7850/3930/4080	Hodell et al. 2001	74	Black Sea	Ti	7220	Bahr et al. 2005
54	SW Europe	ΔT	8970/3320	Davis et al. 2003	75	SE Europe	ΔT	8370/7820	Davis et al. 2003
55	NW Europe	ΔT	none	Davis et al. 2003	76	Kola	δ^{18}O	8180/3550	Jones et al. 2004
57	Swiss Alpes	T7	7950/6030	Wick et al. 2003	81	Soreq Cv, Israel	δ^{18}O	7170/4450	Bar-Matthews et al. 1999
58	Swiss Alpes	P	7920	Wick et al. 2003	82	Red Sea	δ^{18}O	9090/3730	Seeberg-Elverfeldt et al. 2004
59	Swiss Alpes	P	7920/5980	Wick et al. 2003	93	NW Siberia	T7	none	Hantemirov and Shiyatov 2002
60	C Italy	Mg/Ca T	5950/3270	Drysdale et al. 2006	129	Lk Ioannina, Greece	δ^{18}O	4050	Frogley and Griffiths 2001
62	C Italy	δ^{18}O	5950	Drysdale et al. 2006	132	Lk Acigöl, Turkey	δ^{18}O	3160	Roberts et al. 2008
63	S Germany	δ^{18}O	8130/8050/7190	von Grafenstein et al. 1998	133	Lk Frassino, Italy	δ^{18}O	none	Roberts et al. 2008
67	Sweden	GSD	9180/8350 7700/3760	Rubensdotter and Rosqvist 2003	134	Lk Gölhisar, Turkey	δ^{18}O	3070	Roberts et al. 2011

persal or migration. The model is described in more detail in the supporting online material.

Our climate event data base is used to impose sudden reductions (f) of the land utility whenever a climate event occurs in a simulation region. If a local simulated population experiences reduced food yield during a climate event, people attempt to mitigate the crisis by moving to adjacent regions. In this respect, climate events act as a stimulus to migration in the model. If outmigration is not possible, population density declines; with severe population decline, also some of the technologies are lost (Lemmen and Wirtz, 2010).

The simulation is started at 9500 sim BC[1]. All of the 685 biogeographically defined regions are initially set with farming activity at 4% and established agropastoral communities at 25%, what represents a low density Mesolithic technology population and a broad spectrum foraging lifestyle with low unintentional farming activity. We define a local population as Neolithic when the share of agropastoralists is larger than the share of foragers—regardless of its technology, economic diversity, or population density (Figure 2). Experiments are performed with different impact strength (f) of extreme events on land utility to assess climate related sensitivities; here we compare the simulation without climate events ($f = 0\%$) to simulations where the utility reduction was $f = 10\%$ to 100%; results are shown for $f = 40\%$, a value that represents a moderate but not excessive impact.

2.3. Reference data

Our reference is a sub-set of the comprehensive data collection by Pinhasi et al. (2005), who used site data provided by the United Kingdom Archaeology Data Service, the Central Anatolian Neolithic e-Workshop (CANeW),

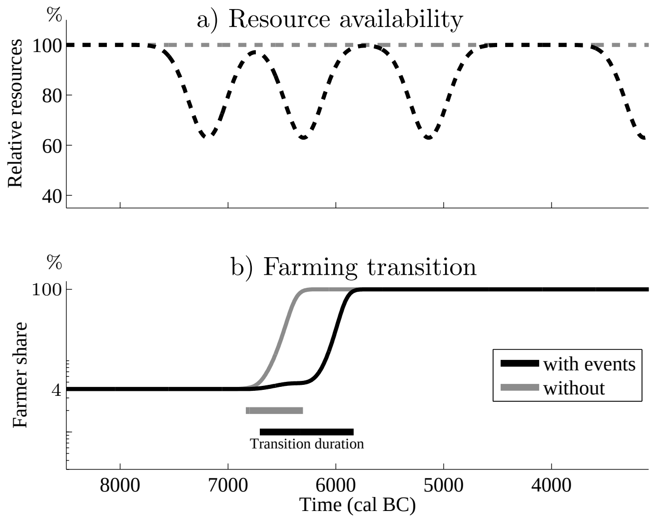

Figure 2: Simulated climate events and evolution of farmer share for an example region. (a, top) Declining resource availability at times where the palaeoclimate record indicates climate extremes. (b, bottom) Transition from hunting-gathering to agropastoralism in the simulation without (grey) and with (black) climate events. Both the timing of the transition as well as the duration of the transition (defined as the time needed in the simulation to increase the farmer share from 4.1% to 95%) are prolonged by the introduction of climate events in this example region.

the radiocarbon CONTEXT database, and the Radiokarbondaten Online (RADON) database. In their compilation, Pinhasi et al. included only sites with small dating uncertainty (≤ 200 a) and report dates based on calibration of original ^{14}C measurements with CalPal 2004. The data set contains dates distributed across Western Eurasia and was recommended by its authors for comparison with simulation studies (see Figure 3 for dates and locations). For numerical comparison with the simulation, we calculate the timing of the Neolithic onset from the radiocarbon date of all sites located within each simulation region. As there is no standard procedure for calculating such an area-

[1]we use the age scale 'simulated time BC' (sim BC) to distinguish between empirically determined age models (cal BC) and the simulation time scale

averaged onset (Müller, 2000), we us the average date.

3. Results

In the reference GLUES simulation including climate variability, farming originates in the Fertile Crescent and southeast Europe in the 7th millennium sim BC and penetrates into Europe in a northwest direction (Figure 3). By 3500 sim BC all of continental Europe has converted to farming as the predominant subsistence style.

3.1. Expansion of agropastoralism

The initial development progresses slowly and at a low level. It begins during the 67th century sim BC in the Levant and Greece[2], followed by the central Balkan (66th century). From these centers, farming spreads to the western Black Sea coast during the 62nd century, and is present throughout the entire Balkan, Anatolia, and Mesopotamia by the 59th century. In these areas, the northward spread of farming stagnates, while farming activity intensifies up to the 56th century on the Balkan, and while farming expands to Italy and the eastern Black Sea coast.

From the 55th to the 59th century sim BC, a rapid expansion through central Europe—or what is archaeologically seen as the Linearbandkeramik area—is simulated, such that farming is the major subsistence style throughout central and southeastern Europe, including the the northern Black Sea coast. From the 46th century, farming emerges along the Baltic Sea coast, and has become the dominant subsistence style throughout the North European plains, Poland, and Denmark by the 42nd century. In France and England, first farming is evident from the 39th century.

Independently, farming also originates in North Africa at the Gibraltar Strait in the 61st century sim BC, from where it spreads into Morocco and the Iberian peninsula, penetrating southern Spain and Morocco by the 54th century. The expansion into northern Iberia stagnates until the 49th century; and slowly connects along the Mediterranean coast to the Fertile Crescent expansion branch by the 46th century. All of of the Iberian peninsula has converted to farming by the 42nd century. By the 34th century, all of continental western Eurasia and England rely almost exclusively on farming. An animation showing the expansion of agriculture into Europe is shown as a supplementary Movie S1.

While the simulation captures the eastern route of the Neolithic into Europe (via Greece, the Balkan, Hungary, then north- and westward, see Rasse 2008 for an overview of routes) quite well, it fails to simulate the Mediterranean route (Cyprus, Sicily, French coast, then northward); this was attributed by Lemmen et al. (2011) to the lack of sea transport in the current model. A western route into Europe is suggested by the model emanating from the Strait of Gibraltar; apart from some zooarchaological evidence (Anderung et al., 2005), this route has not been confirmed by archaeology (Gronenborn, 2009; Rasse, 2008).

The regional timing of agropastoralism is contrasted with the median radiocarbon dates of Neolithic sites compiled by Pinhasi et al. (2005) (Figure 3). From this synoptic, time-integrated perspective, the simulated centers of agropastoralism in the Fertile Crescent, in northern Greece and at the Strait of Gibraltar are evident, as well as the southeast to northwest temporal gradient of the Neolithic transition. The general pattern of the simulated transition resembles the pattern that can be seen from the radiocarbon dates; locally, many dates deviate from the large-scale simulation or disagree with each other within a simulation region.

Overall, the model skill visualized in Figure 4 indicates that recorded variability both between and within European regions can be sufficiently well reproduced by the combination of migration and endogenous dynamics as formulated in GLUES. There is a significant correlation between the hindcasted onsets and the reconstructed onset in both the simulation with and without climate events ($r^2 = .37, r^2 = .43, n = 39, p > .99$, respectively). The simulation with climate events hindcasts the onset for most regions 162 years later than the average reconstructed onset; the mean model bias is $\approx 400 \pm 1000$ years; the difference to the simulation without climate events (median onset 282 years earlier than the reconstruction) is statistically not significant.

On average, climate events delay the onset by 461 ± 179 years. Small delays (minimum 65 years) occur in regions where climate events are temporally separated from the transition, while long delays (maximum 1150 years) occur in regions where several climate events occur shortly before and in the initial phase of the transition. Climate events during the transition tend to prolong the duration of the transition by 50–100 years but this trend is not statistically significant.

4. Discussion

4.1. Stagnation lines in model and archaeological evidence

The Global Land Use and technological Evolution Simulator is able to hindcast a realistic spatiotemporal pattern of the introduction of farming and herding into Europe between 7000 and 3500 sim BC. Simulated transitions towards agropastoralism compare well to a large dataset of radiocarbon dated Neolithic sites. In the simulation, as well as in the data, agropastoralism did not expand uniformly, but rather in periods of rapid spread interrupted by periods of spatial stagnation—but local intensification. This rapid Neolithization, for example, applies to the expansion from Greece to the central Balkan in the 67th century sim BC, which is followed by a 400 a period of relative stagnation. A very similar pattern is hindcasted for

[2]We use current geographic names to refer to the simulation regions

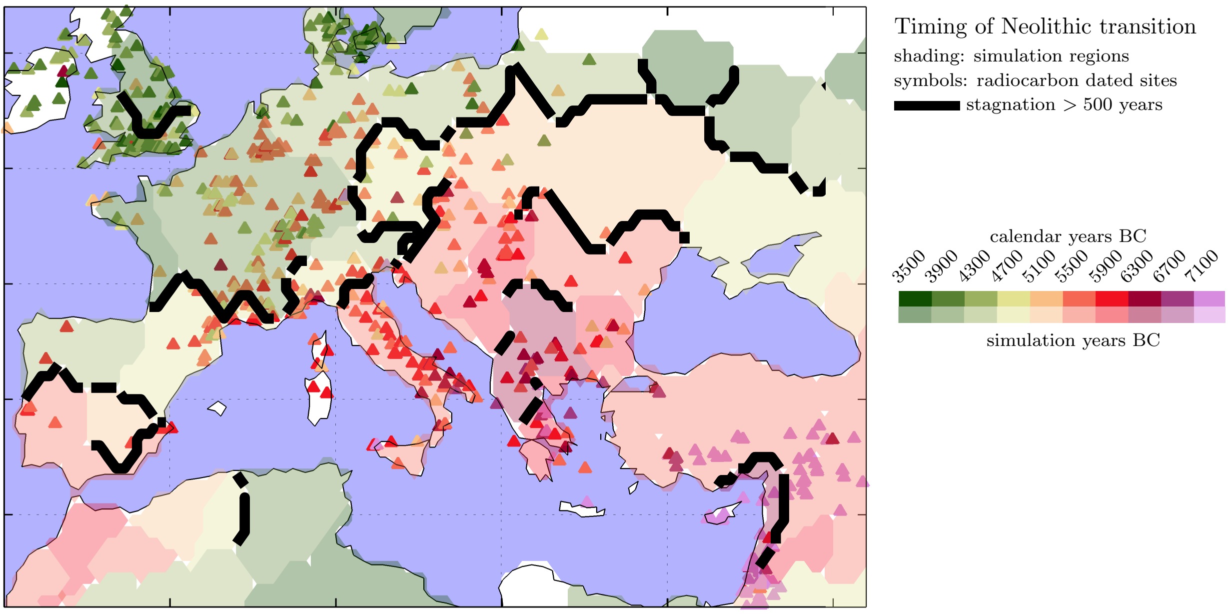

Figure 3: Timing of the transition to agropastoralism in Western Eurasia. The simulated transition (background pastel shading) is contrasted with the radiocarbon ages of Neolithic sites from Pinhasi et al. (2005, solid color triangles). Bold lines indicate regional stagnation periods where the onset lag between neighboring regions is at least 500 years.

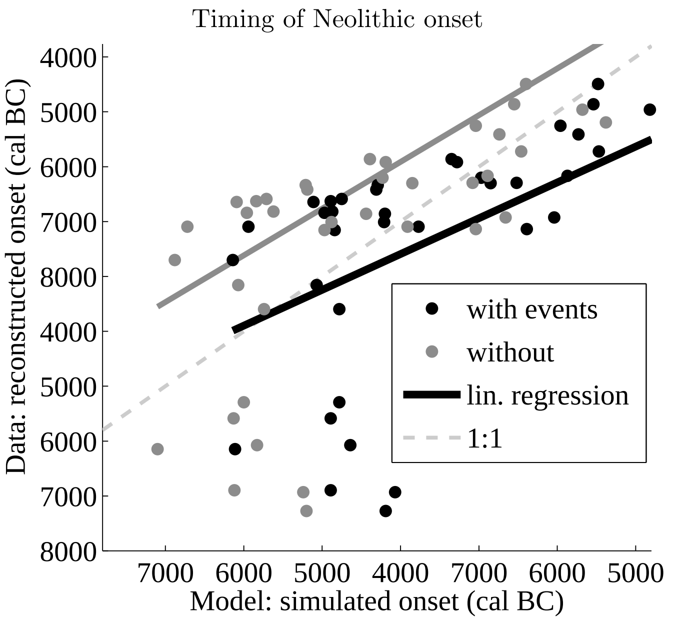

Figure 4: Reconstructed timing of agropastoralism versus simulated onset using a constant or a fluctuating climate forcing (grey and black circles, respectively). The lower left cluster of outliers represents Fertile Crescent and Anatolian founder regions.

the Linearbandkeramik-like Neolithization in the 55th and 54th century cal BC, and for the relative stagnation before the onset of a Funnelbeaker-like cultural complex further north, in the 49th to 46th century. Other stagnation lines identified in the model occur around the Levant and along the Pyrenees, and divide the southern from the northern Iberian peninsula.

These stagnation periods were archaeologically recognized in Guilaine's (2003) 'hypothèse arythmique'. Based on this hypothesis, Rasse (2008) identified stagnation lines by analyzing isolines in the European Neolithic radiocarbon record: he also found long duration stagnation lines running through Iberia and the Pyrenees, and one crossing Anatolia; shorter stagnation lines were identified in Greece, one bisecting the Balkan, another running along the Carpathian mountains, and one along the Alps. Extending the earlier work, Schier (2009) emphasized a major stagnation line along the northern edge of the European loess belt, separating the Linearbandkeramik and Funnelbeaker cultures between 5100 and 4400 cal BC.

Dispersal models of the European Neolithic create spatial structure in the simulated Neolithization pattern from geographic and topographic constraints (e.g. Davison et al., 2006; Ackland et al., 2007; Galeta et al., 2011). We add to this infrequent climate excursions emerging as sudden decreases of the natural productivity and diffusion rates of traits and people. This diffusion not only depends on the topography and geography, but again on (simulated) people and their technology. Compared to those dispersal studies, our model draws a more heterogeneous picture of the regional transitions to agriculture; it is the only model which is capable of representing stagnations in the expansion. We are thus one step further in establishing a simulation of the deterministic pattern of the Neolithic in Europe. Where this deterministic pattern fails to reproduce archaeological information, we can in the future more precisely identify times and regions where human agency played a dominant role.

Before the discrepancies can be exploited scientifically, several caveats about the simulation have to be considered: (1) the model deviation is larger than the uncertainty associated with radiocarbon dates for most sites. (2) each simulation region covers a large area which cannot be fully represented by individual sites, such that the scale difference introduces an additional comparison uncertainty; (3) there is a a spatial bias in the data: the number of sites per simulation region varies, and there is good coverage along the transect from the Levant to northwestern Europe, but few or no information on eastern Europe, on the Iberian peninsula, and in North Africa.

4.2. Role of climate events

Reconstructed climate events episodically depressed population density and to a lesser extent technological stages. The impact of events on the timing of the Neolithic simulation is largest whenever they occurred before or during the first stage (between 10–50% agropastoralists) of a local transition: In 29 regions (out of the 53 simulation regions in Europe), a climate event occurred during the transition. On average, the transition was delayed by 50–100 years (w.r.t. a simulation without events). In three cases, a regionally emerging agropastoral life style reverted back to hunting and gathering during a climate event.

Not everywhere, however, where a climate event coincides with the transition, there is a delay; and vice versa, there are delays in regions which did not experience climate events during the transition to agriculture, such as in most parts of western central Europe. All individual regions are closely connected by neighbor and remote trade relations: impacts, such as those of climate events, may have had far-reaching consequences beyond the locally affected region (Weninger et al., 2005).

As evident from comparing this study with the one by Lemmen et al. (2011), climate fluctuations hindered the development in Greece and the Balkan (which is now more realistic), while the temporal gaps between the central Balkan, the Linearbandkeramik culture, and the Funnelbeaker regions become more pronounced, which is also more consistent with archaeological evidence (Pinhasi et al., 2005; Barker, 2006; Schier, 2009). Compared to the field evidence, the simulation shown here is too late in reproducing the transition to farming in France. Though migration is not enhanced by climatic triggers in continental Europe, it does increase so for Great Britain, where the transition occurs as early as France thanks to increased immigration.

The differences we obtain between simulated timing and the radiocarbon age of related sites (Figures 3) indicate a partial improvement over the simulation without climate events shown by Lemmen et al. (2011): the overall bias of the simulation increased slightly (the event forcing led to an overall delay of the onset), but the variability in the data could be redrawn more precisely. Despite the non-significant regressions between reconstructed and hindcasted onsets and durations of the Neolithic, the scatter alignment is close to the 1:1 line—apart from a bias in the onset hindcasts for the Levante regions (Figure 4); neither regionally clumped chronologies nor model assumptions can be expected to be quantitatively precise.

Overall, uncertainties in the simulated timing, the radiocarbon dates, and in the regional up-scaling are yet so large, that the differences between the simulation with and without climate events are not statistically significant for Europe. Yet, the reconstruction of climate events improved the hindcasted Neolithic transition, both in timing and regional transition durations. On the one hand, this points to an effective albeit limited sensitivity of societal dynamics to environmental shifts. On the other hand, this result supports the notion of a large resilience of cultures, just like Grosman (2003) found for the Late Natufians. Agency, the capacity of cultural complexes to adapt and preserve their life-styles still appears as the dominant model for understanding past human ecodynamics.

This short paper is only a start in the direction of tackling the climate-culture link on large scales, and it gives a perspective of what could be achieved by bringing palaeoclimate data, cultural modeling, and chronologies together. The idealization of climate events we present here needs to be discussed and evaluated further, likewise the (few) assumptions made by the model. In this attempt, the increasing availability of local chronologies will stimulate regional-scale simulation studies for Europe and other continents.

5. Conclusion

We presented a spatially explicit mathematical model of the Neolithization of western Eurasia from 7000 BC to 3500 BC. Our model incorporates endogenous sociotechnological dynamics, as represented by the adaptation of characteristic population traits and their interaction with demographics and changing environments. The simulation improved in hindcasting the Neolithic expansion after integrating quasi-realistic climate events, especially with regard to stagnation phases visible also in field data. This outcome helps to confine the relevance of climate variability in influencing past human ecodynamics and suggests a dominance of endogenous over exogenous control factors.

Acknowledgments

We acknowledge the financial support for C.L. by the German National Science Foundation (DFG priority project Interdynamik 1266), and for both authors by the PACES programme of the Helmholtz society (HGF). We thank the editor and anonymous reviewer for thoughtful comments on an earlier version of this manuscript. This work would not be possible without the many data contributors who made their data publicly available or provided it to us for analysis, thank you.

Supporting material

In the supporting online material, a movie of the expansion of agriculture (Movie S1), the full table of globally distributed palaeoclimate time series (Table S1), and a more detailed description of GLUES are available. The simulated data have been permanently archived on and are freely accessible from PANGAEA (Data Publisher for Earth & Environmental Science) as a netCDF dataset with reference doi:10.1594/PANGAEA.779660. GLUES is free and open source software and can be downloaded from http://glues.sourceforge.net.

References

Ackland, G. J., Signitzer, M., Stratford, K., Cohen, M. H., May 2007. Cultural hitchhiking on the wave of advance of beneficial technologies. Proceedings of the National Academy of Sciences of the United States of America 104 (21), 8714–9.

Ammerman, A. J., Cavalli-Sforza, L. L., 1971. Measuring the Rate of Spread of Early Farming in Europe. Man 6 (4), 674–688.

Anderung, C., Hellborg, L., Elburg, R., Go, A., Smith, C., Bradley, D. G., Ellegren, H., Götherström, A., Nov. 2005. Cattle domestication in the Near East was followed by hybridization with aurochs bulls in Europe. Proceedings of the Royal Society B 272 (1579), 2345–50.

Bahr, A., Lamy, F., Arz, H. W., Kuhlmann, H., Wefer, G., Feb. 2005. Late glacial to Holocene climate and sedimentation history in the NW Black Sea. Marine Geology 214 (4), 309–322.

Balaresque, P., Bowden, G. R., Adams, S. M., Leung, H.-Y., King, T. E., Rosser, Z. H., Goodwin, J., Moisan, J.-P., Richard, C., Millward, A., Demaine, A. G., Barbujani, G., Previderè, C., Wilson, I. J., Tyler-Smith, C., Jobling, M. a., Jan. 2010. A predominantly Neolithic origin for European paternal lineages. Public Library of Science Biology 8 (1), e1000285.

Bar-Matthews, M., Ayalon, A., Kaufman, A., Wasserburg, G. J., 1999. The Eastern Mediterranean paleoclimate as a reflection of regional events: Soreq cave, Israel. Earth and Planetary Science Letters 166 (1-2), 85–95.

Barker, G., 2006. The Agricultural Revolution in Prehistory. Why did Foragers become Farmers? Oxford University Press, Oxford, United Kingdom.

Berger, J.-F., Guilaine, J., May 2009. The 8200 cal BP abrupt environmental change and the Neolithic transition : A Mediterranean perspective. Quaternary International 200 (1-2), 31–49.

Berglund, B. E., 2003. Human impact and climate changes–synchronous events and a causal link? Quaternary International 105 (1), 7–12.

Bocquet-Appel, J.-P., 2008. Explaining the Neolithic Demographic Transition. In: Bocquet-Appel, J.-P. (Ed.), The Neolithic Demographic Transition and its Consequences. Springer, Berlin Berlin / Heidelberg, pp. 35–55.

Bond, G., Nov. 1997. A Pervasive Millennial-Scale Cycle in North Atlantic Holocene and Glacial Climates. Science 278 (5341), 1257–1266.

Bond, G., Kromer, B., Beer, J., 2001. Persistent solar influence on North Atlantic climate during the Holocene. Science 294 (5549), 2130–2136.

Chapman, M., Shackleton, N., May 2000. Evidence of 550-year and 1000-year cyclicities in North Atlantic circulation patterns during the Holocene. The Holocene 10 (3), 287–291.

Childe, V. G., 1925. Dawn Of European Civilization, 1st Edition. History of Civilization. Routledge [reprinted 2005].

Childe, V. G., 1942. What happened in history. Pelican/Penguin, Harmondsworth.

Coombes, P., Barber, K., 2005. Environmental determinism in Holocene research: causality or coincidence ? Area 37 (3), 303–311.

Cullen, H. M., DeMenocal, P. B., Hemming, S., 2000. Climate change and the collapse of the Akkadian empire: Evidence from the deep sea. Geology 28 (4), 379–382.

Dakos, V., Scheffer, M., 2008. Slowing down as an early warning signal for abrupt climate change. Proceedings of the National Academy of Sciences of the United States of America 105 (38), 14308–14312.

Davis, B. A. S., Brewer, S., Stevenson, A. C., Guiot, J., Jul. 2003. The temperature of Europe during the Holocene reconstructed from pollen data. Quaternary Science Reviews 22 (15-17), 1701–1716.

Davison, K., Dolukhanov, P. M., Sarson, G. R., Shukurov, A., May 2006. The role of waterways in the spread of the Neolithic. Journal of Archaeological Science 33 (5), 641–652.

de Vries, H. J. M., Thompson, M., Wirtz, K. W., 2002. Understanding: fragments of a unifying perspective. In: de Vries, H. J. M., Goudsblom, J. (Eds.), Mappae Mundi. Holland Society for Arts and Science, Haarlem, pp. 257–299.

DeMenocal, P. B., 2001. Cultural responses to climate change during the late Holocene. Science 292 (5517), 667–673.

DeMenocal, P. B., Ortiz, J., Guilderson, T., Adkins, J., Sarnthein, M., Baker, L., Yarusinsky, M., 2000. Abrupt onset and termination of the African Humid Period: rapid climate responses to gradual insolation forcing. Quaternary science reviews 19 (1-5), 347–361.

Dolukhanov, P. M., 1973. The Neolithisation of Europe: a chronological and ecological approach. In: Renfrew, C. (Ed.), The explanation of culture change: models in prehistory. Gerald Duckworth and Co, Gloucester Crescent, pp. 329–342.

Drysdale, R., Zanchetta, G., Hellstrom, J., Maas, R., Fallick, A., Pickett, M., Cartwright, I., Piccini, L., 2006. Late Holocene drought responsible for the collapse of Old World civilizations is recorded in an Italian cave flowstone. Geology 34 (2), 101–104.

Erickson, C. L., 1999. Neo-environmental determinism and agrarian "collapse" in Andean prehistory. Antiquity 73 (281), 634–642.

Feynman, J., Ruzmaikin, A., Apr. 2007. Climate stability and the development of agricultural societies. Climatic Change 84 (3-4), 295–311.

Finné, M., Holmgren, K., Sundqvist, H. S., Weiberg, E., Lindblom, M., Dec. 2011. Climate in the eastern Mediterranean, and adjacent regions, during the past 6000 years A review. Journal of Archaeological Science 38 (12), 3153–3173.

Flannery, K. V., 1973. The Origins of Agriculture. Annual Review of Anthropology 2 (1), 271–310.

Frogley, M., Griffiths, H., 2001. Historical biogeography and Late Quaternary environmental change of Lake Pamvotis, Ioannina (northwestern Greece): evidence from ostracods. Journal of Biogeography 28 (6), 745–756.

Galeta, P., Sládek, V., Sosna, D., Bruzek, J., Jul. 2011. Modeling Neolithic dispersal in Central Europe: Demographic implications. American Journal of Physical Anthropology 146 (1), 104–115.

Gasse, F., 2000. Hydrological changes in the African tropics since the Last Glacial Maximium. Quaternary Science Reviews 19 (1), 189–211.

Gignoux, C. R., Henn, B. M., Mountain, J. L., Apr. 2011. Rapid, global demographic expansions after the origins of agriculture. Proceedings of the National Academy of Sciences of the United States of America 108 (15), 6044–9.

Gronenborn, D., 2009. Transregional culture contacts and the neolithization process in Northern Central Europe. In: Jordan, P., Zvelebil, M. (Eds.), Ceramics before farming: the dispersal of pottery among prehistoric Eurasian hunter-gatherers. Left Coast Press, Walnut Creek, CA, pp. 527–550.

Gronenborn, D., 2010. Climate, crises and the "Neolithisation" of Central Europe between IRD-events 6 and 4. In: Gronenborn, D., Petrasch, J. (Eds.), Die Neolithisierung Mitteleuropas. Vol. 4(1). Römisch-Germanisches Zentralmuseum, Mainz, pp. 61–80.

Grosman, L., 2003. Preserving cultural Traditions in a period of Instability: The Late Natufian of the Hilly Mediterranean Zone. Current Anthropology 44 (4), 571–580.

Guilaine, J., 2003. De la vague à la tombe. Editions du Seuil, Paris.

Hantemirov, R. M., Shiyatov, S. G., 2002. A continuous multimillennial ring-width chronology in Yamal, northwestern Siberia. The Holocene 12 (6), 717–726.

Hodell, D. A., Curtis, J. H., Sierro, F. J., Raymo, M. E., 2001. Correlation of late Miocene to early Pliocene sequences between the Mediterranean and North Atlantic. Paleoceanography 16 (2), 164–178.

Holmgren, K., Lee-Thorp, J. a., Cooper, G. R., Lundblad, K., Partridge, T. C., Scott, L., Sithaldeen, R., Siep Talma, A., Tyson, P. D., Nov. 2003. Persistent millennial-scale climatic variability over the past 25,000 years in Southern Africa. Quaternary Science Reviews 22 (21-22), 2311–2326.

Husum, K., Hald, M., Nov. 2004. A continuous marine record 80001600 cal. yr BP from the Malangenfjord, north Norway: foraminiferal and isotopic evidence. The Holocene 14 (6), 877–887.

Janssen, M. A., Scheffer, M., 2004. Overexploitation of Renewable Resources by Ancient Societies and the Role of Sunk-Cost Effects. Ecology and Society 9 (1), 6.

Jones, V., Leng, M. J., Solovieva, N., Sloane, H., Tarasov, P. E., 2004. Holocene climate of the Kola Peninsula; evidence from the oxygen isotope record of diatom silica. Quaternary Science Reviews 23 (7-8), 833–839.

Kaplan, J. O., Krumhardt, K. M., Ellis, E. C., Ruddiman, W. F., Lemmen, C., Klein Goldewijk, K., Dec. 2011. Holocene carbon emissions as a result of anthropogenic land cover change. The Holocene 21 (5), 775–791.

Lemmen, C., 2010. World distribution of land cover changes during Pre- and Protohistoric Times and estimation of induced carbon releases. Géomorphologie : relief, processus, environnement 4 (2009), 303–312.

Lemmen, C., 2012. Different mechanisms shaped the transition to farming in Europe and the North American Woodland. Archaeology, Ethnology and Anthropology of Eurasia submitted, 9.

Lemmen, C., Gronenborn, D., Wirtz, K. W., 2011. A simulation of the Neolithic transition in Western Eurasia. Journal of Archaeological Science 38 (12), 3459–3470.

Lemmen, C., Khan, A., 2012. A simulation of the Neolithic transition in the Indus valley. In: Fuller, D. Q. (Ed.), Past Climate, Humans and Landscapes. Vol. in press. American Geophysical Union, p. 6.

Lemmen, C., Wirtz, K. W., 2010. Socio-technological revolutions and migration waves: re-examining early world history with a numerical model. In: Gronenborn, D., Petrasch, J. (Eds.), The Spread of the Neolithic to Central Europe. Vol. 4,1 of RGZM Tagungen. Verlag des Römisch-Germanischen Zentralmuseums, Mainz, pp. 25–38.

Mayewski, P. A., Rohling, E. J., Stager, J. C., Karlén, W., Maasch, K. A., Davidmeeker, L., Meyerson, E., Gasse, F., Vankreveld, S., Holmgren, K., Nov. 2004. Holocene climate variability. Quaternary Research 62 (3), 243–255.

McDermott, F., 2004. Palaeo-climate reconstruction from stable isotope variations in speleothems : a review. Quaternary Science Reviews 23 (7-8), 901–918.

Müller, J., 2000. Zur räumlichen Darstellung von Radiokarbondaten : Zwei Beispiele aus dem Endneolithikum. In: Müller, J. (Ed.), www.jungsteinSITE.de. Vol. 7. Februar. Institut für Ur- und Frühgeschichte, Christian-Albrechts-Universität, Kiel, p. 8.

Peltenburg, E., Colledge, S., Croft, P., Jackson, A., McCarteney, C., Mary, Murray, A., Dec. 2000. Agro-pastoralist colonization of Cyprus in the 10th millennium BP: initial assessments. Antiquity 77 (286), 844–853.

Perlès, C., 2001. The Early Neolithic in Greece: the first farming communities in Europe. Cambridge World Archaeology. Cambridge University Press, Cambridge, United Kingdom.

Pinhasi, R., Fort, J., Ammerman, A. J., 2005. Tracing the origin and spread of agriculture in Europe. Public Library of Science Biology 3 (12), e410.

Rasse, M., 2008. La diffusion du Néolithique en Europe (7000-5000 av. J.-C.) et sa représentation cartographique. M@ppemonde 90 (2), 1–22.

Renfrew, C. (Ed.), 1987. Archaeology and Language. The Puzzle of Indo-European Origins. Jonathan Cape Ltd.

Roberts, N., Eastwood, W. J., Kuzucuoglu, C., Fiorentino, G., Caracuta, V., Jan. 2011. Climatic, vegetation and cultural change in the eastern Mediterranean during the mid-Holocene environmental transition. The Holocene 21 (1), 147–162.

Roberts, N., Jones, M., Benkaddour, A., Eastwood, W. J., Filippi, M., Frogley, M., Lamb, H., Leng, M. J., Reed, J., Stein, M., Stevens, L., Valero-Garcés, B., Zanchetta, G., Dec. 2008. Stable isotope records of Late Quaternary climate and hydrology from Mediterranean lakes: the ISOMED synthesis. Quaternary Science Reviews 27 (25-26), 2426–2441.

Rosen, A. M., Rivera-Collazo, I., Mar. 2012. Climate change, adaptive cycles, and the persistence of foraging economies during the late Pleistocene/Holocene transition in the Levant. Proceedings of the National Academy of Sciences of the United States of America online, 6.

Rubensdotter, L., Rosqvist, G., 2003. The effect of geomorphological setting on Holocene lake sediment variability, northern Swedish Lapland. Journal of Quaternary Science 18 (8), 757–767.

Schier, W., Jan. 2009. Extensiver Brandfeldbau und die Ausbreitung der neolithischen Wirtschaftsweise in Mitteleuropa und Südskandinavien am Ende des 5. Jahrtausends v. Chr. Praehistorische Zeitschrift 84 (1), 15–43.

Schulting, R. J., Oct. 2010. Holocene environmental change and the Mesolithic-Neolithic transition in north-west Europe: revisiting two models. Environmental Archaeology 15 (2), 160–172.

Seeberg-Elverfeldt, I., Lange, C. B., Arz, H. W., Pätzold, J., Pike, J., Aug. 2004. The significance of diatoms in the formation of laminated sediments of the Shaban Deep, Northern Red Sea. Marine Geology 209 (1-4), 279–301.

Shanks, M., Tilley, C., 1987. Re-constructing Archaeology: Theory and Practice. New Studies in Archaeology. Cambridge University Press, Cambridge, United Kingdom.

Sheridan, J. A., 2007. Scottish beaker dates: the good, the bad and the ugly. In: From Stonehenge to the Baltic: Living with Cultural Diversity in the Third Millennium BC. British Archaeological Reports. Archaeopress, Oxford, pp. 91–123.

Smith, S. L., Pahlow, M., Merico, A., Wirtz, K. W., 2011. Optimality-based modeling of planktonic organisms. Limnology and Oceanography 56 (6), 2080–2094.

Sperling, M., Schmiedl, G., Emeis, K. C., Erlenkeuser, H., Grootes, P. M., 2003. Black Sea impact on the formation of eastern Mediterranean sapropel S1? Evidence from the Marmara Sea. Palaeogeography, Palaeoclimatology, Palaeoecology 190 (1), 9–21.

Thomson, D. J., Apr. 1990. Time Series Analysis of Holocene Climate Data. Philosophical Transactions of the Royal Society A: Mathematical, Physical and Engineering Sciences 330 (1615), 601–616.

van der Leeuw, S. E., 2008. Climate and Society : Lessons from the Past 10000 years. Ambio 37 (14), 476–482.

von Grafenstein, U., Erlenkeuser, H., Müller, J., Jouzel, J., Johnsen, S. J., 1998. The cold event 8200 years ago documented in oxygen isotope records of precipitation in Europe and Greenland. Climate Dynamics 14 (2), 73–81.

Wanner, H., Beer, J., Crowley, T., Oct. 2008. Mid-to Late Holocene climate change: an overview. Quaternary Science Reviews 27 (19-20), 1791–1828.

Weiss, H., Courty, M.-A., Wetterstrom, W., Guichard, F., Senior, L., Meadow, R., Curnow, A., Aug. 1993. The Genesis and Collapse of Third Millennium North Mesopotamian Civilization. Science 261 (5124), 995–1004.

Weninger, B., Alram-Stern, E., Clare, L., Danzeglocke, U., Jöris, O., Kubatzki, C., Rollefson, G., Todorova, H., 2005. Die Neolithisierung von Südosteuropa als Folge des abrupten Klimawandels um 8200 Cal B.P. In: Gronenborn, D. (Ed.), Climate Variability and Cultural Change in Neolithic societies of Central Europe, 6700-2200 cal BC. Vol. 1 of RGZM-Tagungen. Römisch-Germanisches Zentralmuseum, Mainz, Germany, pp. 75–118.

Weninger, B., Clare, L., Rohling, E. J., Bar-Yosef, O., Böhner, U., Budja, M., Bundschuh, M., Feurdean, A., Gebel, H.-G., Jöris, O., Linstädter, J., Mayewski, P. A., Mühlenbruch, T., Reigruber, A., Rollefson, G., Schyle, D., Thissen, L., Todorova, H., Zielhofer, C., 2009. The impact of rapid climate change on prehistoric societies

during the Holocene in the Eastern Mediterranean. Documenta Praehistorica 902 (4-5), 551–583.
Whittle, A., Cummings, V. (Eds.), 2007. Going Over: The Mesolithic-Neolithic Transition in North-West Europe. Vol. 144. Oxford University Press.
Wick, L., Lemcke, G., Sturm, M., 2003. Evidence of Lateglacial and Holocene climatic change and human impact in eastern Anatolia: high-resolution pollen, charcoal, isotopic and geochemical records from the laminated sediments of Lake Van, Turkey. The Holocene 13 (5), 665–675.
Wirtz, K. W., Lemmen, C., 2003. A global dynamic model for the neolithic transition. Climatic Change 59 (3), 333–367.
Wirtz, K. W., Lohmann, G., Bernhardt, K., Lemmen, C., Dec. 2010. Mid-Holocene regional reorganization of climate variability: Analyses of proxy data in the frequency domain. Palaeogeography, Palaeoclimatology, Palaeoecology 298 (3-4), 189–200.
Zapata, L., Peña Chocarro, L., Pérez-Jordá, G., Stika, H.-P., Dec. 2004. Early Neolithic Agriculture in the Iberian Peninsula. Journal of World Prehistory 18 (4), 283–325.
Zeder, M. a., Aug. 2008. Domestication and early agriculture in the Mediterranean Basin: Origins, diffusion, and impact. Proceedings of the National Academy of Sciences of the United States of America 105 (33), 11597–604.
Zohary, D., Hopf, M., 1993. Domestication of plants in the old world, 1st Edition. Oxford University press, Oxford, United Kingdom.

Supplementary material for "On the sensitivity of the simulated European Neolithic transition to climate extremes"

Carsten Lemmen*, Kai W. Wirtz

Helmholtz-Zentrum Geesthacht, Institut für Küstenforschung, Max-Planck Straße 1, 21501 Geesthacht, Germany

1. Supplementary information on GLUES

The Global Land Use and technological Evolution Simulator (GLUES, Wirtz and Lemmen, 2003; Lemmen, 2010; Lemmen and Wirtz, 2010) mathematically resolves the dynamics of human populations and their characteristic sociocultural traits in the context of a changing biogeographical environment. A local sociocultural coevolution is described by changes in mean population density (P), technology (T), share of agropastoral activities (Q), and economic diversity (N), within a simulation region of approximately country-size extent (Figure 1 of main manuscript). Each region's population utilises its natural resources, which are described by environmental utility (FEP) and climate constraints (TLI). While the mathematical implementation is summarised in its entirety from Wirtz and Lemmen (2003), the reader is advised to refer to the original manuscript for detailed motivation for each model assumption.

1.1. Characteristic trait dynamics

For pre-industrial human societies, Wirtz and Lemmen (2003) defined three characteristic traits $X \in \{\mathrm{T}, \mathrm{Q}, \mathrm{N}\}$:

1. Technology (T) is a trait which describes the efficiency of food procurement related to both foraging and farming.
2. A second model variable (Q) describes the allocation of energy, time, or manpower to agropastoralism.
3. Economic diversity (N), resolves the number of different economies in the agropastoral sector which are available to a region's population.

The evolution of each of these traits (X) follows the direction of increased benefit for success (i.e., growth benefit $\partial r/\partial X$) of its associated population; this concept had been derived for genetic traits in the works of Fisher (1930), and more recently by Metz and colleagues (e.g. Kisdi and Geritz, 2010) as adaptive dynamics (AD). In AD, the population averaged value of a trait changes at a rate which is proportional to the gradient of the fitness function, evaluated the mean trait value:

$$\frac{\mathrm{d}X}{\mathrm{d}t} = \delta_X \frac{\partial r}{\partial X} \qquad X \in \{\mathrm{T}, \mathrm{Q}, \mathrm{N}\}, \tag{1}$$

where δ_X is the so-called flexibility for trait X and is often given by the variance of X; r denotes the relative growth rate of the population, i.e. $r = (\mathrm{dP}/\mathrm{d}t)/\mathrm{P}$.

1.2. Productivity and growth

The Neolithic transition is characterised by changes in subsistence intensity (SI). Subsistence intensity describes a community's effectiveness in generating consumable food and secondary products; this can be achieved based on an agricultural (with fractional activity Q) and a hunting-gathering life style (with fractional activity $1 - \mathrm{Q}$). SI is dimensionless and scaled such that a value of unity expresses the mean subsistence intensity of a hunter-gatherer society equipped with tools typical for the mature Mesolithic and living in an affluent natural environment.

$$\mathrm{SI} = (1 - \mathrm{Q}) \cdot \sqrt{\mathrm{T}} + \mathrm{Q} \cdot \mathrm{N} \cdot \mathrm{T} \cdot \mathrm{TLI} \tag{2}$$

The agricultural part of SI increases linearly with N and with T: The more economies (N) there are, the better are sub-regional scaled niches utilised and the more reliable returns are generated when annual weather conditions are variable; the higher the technology level (T), the better the efficiency of using natural resources (by definition of T). While a variety of techniques can steeply increase harvests of domesticated species, analogous benefits for foraging productivity are less pronounced and justify a less than linear dependence of the hunting-gathering calorie procurement on T. We use a square root formulation, which satisfies $\sqrt{\mathrm{T}} < \mathrm{T}$ since T is generally larger than unity.

We introduce an additional temperature constraint (TLI) on agricultural productivity which considers that cold temperature could only moderately be overcome by Neolithic technologies. This limitation is unity at low latitudes and approaches zero at permafrost conditions.

The domestication process is represented by N, which is the number of realised agropastoral economies. We link N to natural resources by expressing it as the fraction f of potentially available economies (PAE) by specifying $\mathrm{N} = f \cdot \mathrm{PAE}$, where the latter corresponds to the richness in domesticable animal or plant species within a specific region.

1.3. Food productivity and human growth rate

The growth rate r of a regional population relative to its size is mainly controlled by its subsistence intensity SI:

*Tel +49 4152 87-2013, Fax -2020
Email address: carsten.lemmen@hzg.de (Carsten Lemmen)

$$r = \mu \cdot (\mathrm{FEP} - \gamma\sqrt{\mathrm{T}}\mathrm{P}) \cdot (1 - \omega\,\mathrm{T}) \cdot \mathrm{SI} - \rho \cdot \mathrm{P} \cdot \mathrm{e}^{-\mathrm{T}/\mathrm{T_{lit}}}, \quad (3)$$

with growth rate parameters μ and ρ. The subsistence intensity's contribution to growth is modulated by environmental utility (FEP), societal impacts on the environment ($-\gamma\sqrt{\mathrm{T}}\mathrm{P}$), and organisational losses within a society ($1-\omega\,\mathrm{T}$). As technology advances, more and more people neither farm nor hunt: Construction, maintenance, administration draw a small fraction ω of the workforce away from food-production. The impact on the environment is modelled as a function of population density and technology (IPAT, Ehrlich and Holdren, 1971) on the utility of the environment (FEP, see next section). The loss term is mediated by technologies (T, with $\mathrm{T_{lit}} = 12$), which mitigate, for example, losses due to disease. The implementation of the loss term differs from the originally inverse formulation by Wirtz and Lemmen (2003, $-\rho\frac{\mathrm{P}}{\mathrm{T}}$), but is numerically simpler and phenologically similar.

1.4. Region definition

GLUES operates on a set of regions which, in turn, are defined on a high resolution ($0.5° \times 0.5°$) grid. The region definition is implemented as a Cellular Automaton (CA), and resembles the application of a spatial low-pass filter to the grid. The CA formalism facilitates a dynamisation of region boundaries in future model applications. The CA aims at describing the organisation of local Mesolithic and Neolithic populations as cultural complexes that share common traits across larger spatial scales. The algorithm combines single adjacent cells into a cluster (region), starting from a distribution where each cell forms an individual cluster. The CA iteratively computes the similarity in geographical characteristics between neighbour cells. Similarity is defined as the sum of absolute and normalised differences in discriminating local properties (NPP and growing degree days). The similarities to all neighbour cells are weighted by a factor $A/(A+A_T)$ where A denotes the area of the adjacent cluster and A_T a predefined target cluster size. The neighbour cell with maximal area weighted similarity then inherits cluster membership to the original cell. Cells that together with similar neighbours already form a cluster, usually do not change membership, while cells with a regionally anomalous biogeography become part of a new cluster. As a result, larger clusters incorporate cells at their boundary in relation to their own size and biogeographical similarity. The cluster distribution reaches a steady state when most cells are organised in clusters of relatively large cell number ($A > 2A_T$). Small clusters below the threshold size A_T may, however, persist depending on the topography and the choice of A_T; these are attached to one of the adjacent cluster regions using the area weighted similarity computed at the cluster scale.

1.5. Coupling to biogeography

We reconstruct past distributions of net primary production (NPP) using a global climate model coupled to a vegetation module. From Climber-2 (Claussen and Brovkin, 1999) temperature (t) and precipitation (p) anomalies on the IIASA climatological database (Leemans and Cramer, 1991) we calculated NPP following Lieth (1975, Miami model):

$$\begin{aligned}
\mathrm{NPP}_p &= \left(1 - \mathrm{e}^{-0.664p/\mathrm{m}}\right) \cdot \frac{1460\,\mathrm{g}}{\mathrm{m}^2\,\mathrm{a}} \\
\mathrm{NPP}_t &= \left(1 + 3.7248\,\mathrm{e}^{-0.119t/°\mathrm{C}}\right)^{-1} \cdot \frac{1460\,\mathrm{g}}{\mathrm{m}^2\,\mathrm{a}} \\
\mathrm{NPP} &= \min\left(\mathrm{NPP}_p, \mathrm{NPP}_t\right) \qquad (4)
\end{aligned}$$

Local food extraction potential (FEP) represents the utility of a multidimensional environment for food production; this FEP generally increases with NPP; at very high (i.e. tropical) NPP, it decreases because the amount of non-usable biomass rises (Bloom et al., 1998) and the crop yield declines (Gallup and Sachs, 2000). We choose $\mathrm{NPP}_F = 1100\,\mathrm{g\,m^{-2}\,a^{-1}}$ to describe the productivity where FEP is highest and derive FEP as follows:

$$\mathrm{FEP} = \frac{2\frac{\mathrm{NPP}}{\mathrm{NPP_F}}}{(\frac{\mathrm{NPP}}{\mathrm{NPP_F}})^2 + 1} \qquad (5)$$

According to Braidwood and Braidwood (1949)'s hilly flanks hypothesis, potential domesticates were most abundant in open woodlands, which are characterised by low to moderate NPP; we accordingly use a monomodal transfer function to calculated the relative local potential for agropastoral economies (LAE), with a maximum at $\mathrm{NPP_N} = 550\,\mathrm{g\,m^{-2}\,a^{-1}}$.

$$\mathrm{LAE} = \mathrm{TLI} \cdot \frac{4\frac{\mathrm{NPP}}{\mathrm{NPP_N}}}{(\frac{\mathrm{NPP}}{\mathrm{NPP_N}})^3 + 3} \qquad (6)$$

Temperature limitation is included in the calculation of LAE because cold-adapted plants do generally not carry usable large seeds, fruits or tubers.

Following the concept of, for example, Gaston (2000) for the connection of species richness on two different spatial scales, we connect the relative local potential (LAE) with the continental potential for agropastoral economies (CAE) to obtain an absolute local potential for agriculture (PAE); this way, we also account for continental aggregation area-biodiversity relationships. Let i denote a region index and $\mathcal{I}_k$ the set of regions on continent k. Then

$$\mathrm{PAE}_i = \mathrm{LAE}_i \cdot \mathrm{CAE}_k \qquad \text{for} \qquad i \in \mathcal{I}_k \qquad (7)$$

As continents, we consider seven ($k \in \{1 \ldots 7\}$) large biogeographic units: Australia, Subsaharan Africa, Eurasia including North Africa, North America, South America, Greenland, and one unit consisting of all large islands. To obtain CAE_k, we calculate a weighted sum of all LAE with region area A_i on continent k, and scale with the values for the largest continent (Eurasia) where $\mathrm{CAE}_k = \mathrm{CAE_{max}}$ and $A_k = A_{\mathrm{max}}$. The consideration of region areas A_i represents a linearised species-area relationship (Begon et al., 1993).

$$\mathrm{CAE}_k = \mathrm{CAE}_{\max} \cdot A_{\max}^{-1} \cdot \sum_{i \in \mathcal{I}_k} (A_i \cdot \mathrm{LAE}_i)\,. \tag{8}$$

1.6. Interregional exchange

Exchange between region i and its neighbour j in the neighbourhood $\mathcal{N}_i$ comprises communication, trade, colonisation, warfare, migration of individuals or entire populations. We use the concept of influence by Renfrew and Level (1979), defined by us as the product of P and T to reflect imbalances in population pressure and disparate technologies. Influence differences relative to the spatial average $\langle \mathrm{T} \cdot \mathrm{P} \rangle_{ij}$ act as a driving force f_{ij} for exchange. The flux f_{ij} is formulated as a first order relaxation (e.g. Wang and van Cappellen, 1996) and depends on (1) the influence difference, (2) common boundary length L_{ij} of the two regions, (3) the distance of their centres $\sqrt{A_i A_j}$, and (4) exchange coefficients for spread with peopleσ_{P} and without σ_{T}.

$$f_{ij} = \sigma_{\mathrm{P,T}} \frac{L_{ij}}{\sqrt{A_i A_j}} \cdot (\langle \mathrm{T} \cdot \mathrm{P} \rangle_{ij} - \mathrm{T}_i \mathrm{P}_i) \tag{9}$$

Whenever there is a positive flux $f_{ij} > 0$, trait value differences in traits T and N from its neighbourhood $\mathcal{N}_i$ are added to region i's traits:

$$\left.\frac{\mathrm{d}X_i}{\mathrm{d}t}\right|_{\mathrm{T}} = \sum_{j \in \mathcal{N}_i, f_{ij} > 0} f_{ij} \cdot (X_j - X_i) \tag{10}$$

Population diffusion is mass-conserving and is composed of immigration ($f_{ij} > 0$) and emigration ($f_{ij} < 0$) of individuals or groups.

$$\left.\frac{\mathrm{dP}_i}{\mathrm{d}t}\right|_{\mathrm{P}} = \sum_{j \in \mathcal{N}_i, f_{ij} > 0} f_{ij} \mathrm{P}_j \frac{A_j}{A_i} - \sum_{j \in \mathcal{N}_i, f_{ij} < 0} f_{ij} \mathrm{P}_i \tag{11}$$

With immigrating people, the characteristic traits of the migrants are carried over to the receiving region:

$$\left.\frac{\mathrm{d}X_i}{\mathrm{d}t}\right|_{\mathrm{P}} = \sum_{j \in \mathcal{N}_i, f_{ij} > 0} f_{ij} X_j \frac{\mathrm{P}_j A_j}{\mathrm{P}_i A_i} \tag{12}$$

1.7. Cultural memory loss

When population declines, a cultural loss (loss of technology and applied economies) is imposed on a regional society. This loss is described by Lemmen (2010) and formulated as

$$\left.\frac{\mathrm{d}X_i}{\mathrm{d}t}\right|_{\mathrm{crisis}} = \beta \cdot r \cdot X \tag{13}$$

Where β describes the percentage of knowledge loss at a given relative loss in population number. In this study, we set $\beta = 0.8$

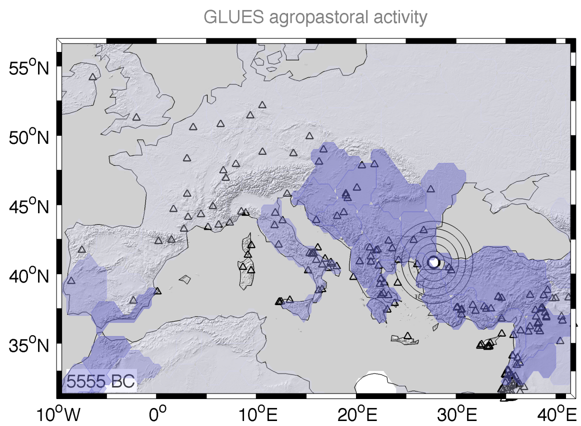

Figure 1: Expansion of farming activity across Europe. Snapshot of the movie (click picture to play) supplied with this supplementary material. Blue shading indicates regions with predominant farming activity; triangles show the location of radiocarbon dated Neolithic archaeological sites; white dots show the location and duration of climate events diagnosed from globally 134 palaeoclimate records.

Table 1: Table of 134 palaeoclimate time series, of which 122 were analysed by Wirtz et al. (2010, their Table 2). Abbreviations: Lk=Lake, Cv=Cave, LG=lithic grains, SST=sea surface temperature, T=temperature, T7=July temperature, P=precipitation, GSD=grayscale density, HSG=hematite stained glass, SSS=sea surface salinity,Ef=effective, LG=lithic grains, Nitz.=Nitzschia, Ozean.=Ozeanica, Ti=Titanium content

No	Site	Proxy	Events (cal BC)	Reference
1	NW Alaska	Mg/Ca T	7370/6530	Hu et al. 1998
2	NW Pacific	δ^{18}O	none	Oba and Murayama 2004
3	Owens Lk, CA	δ^{18}O	9180	Benson et al. 2002
4	E California	P	6910/6390	Hughes and Graumlich 1996
5	W Canada	Density	6950/6230/4680	Yu 2003
6	S California	Moisture	5850	Davis 1992
7	Moon Lk, ND	Salinity	none	Laird et al. 1996
8	Kimble, MN	Charcoal	3010	Camill et al. 2003
9	Sharkey, MN	Charcoal	3970	Camill et al. 2003
10	NC America	δ^{18}O	7470/6530/4670	Denniston et al. 1999
11	Cold Water Cv, IA	δ^{18}O	6730/3550 3290/3020	Dorale et al. 1992
12	Guatemala	δ^{18}O (Cy)	7040/3560	Curtis et al. 1998
13	Guatemala	δ^{18}O (Co)	8950/4520	Curtis et al. 1998
14	Guatemala	δ^{18}O (Py)	9010/3250	Curtis et al. 1998
15	E Pacific	δ^{18}O	none	Rosenthal 2003
16	Yucatan	δ^{18}O (Ph)	none	Hodell et al. 1995
17	Yucatan	δ^{18}O (Py)	none	Hodell et al. 1995
18	Costa Rica	δ^{18}O	7760/3890 7350/6680	Lachniet et al. 2004
19	E Canada	Charcoal	6220/4250	Carcaillet et al. 2001
20	Ecuador	ENSO	9400/3790	Moy et al. 2002
21	E Canada	Charcoal	6550/3690	Carcaillet et al. 2001
22	Ecuador	GSD	none	Rodbell et al. 1999
23	Huascaran, Peru	δ^{18}O	none	Thompson et al. 2003
24	Chile	δ^{18}O	6640/5920/5740	Lamy et al. 2002
25	Chilean Coast	SST	6700/4380	Lamy and Hebbeln 2001
26	Haiti	δ^{18}O	9250/8940 8770/7600	Higuera-Gundy et al. 1999
27	New England	Storms	none	Noren et al. 2002
28	Lk Titikaka	Level	none	Abbott et al. 1997
29	Sajama, Bolivia	Particles	4500/3500	Thompson et al. 2003
30	Sajama, Bolivia	δ^{18}O	4100	Thompson et al. 2003
31	Venezuela	δ^{18}O	7400/6570 5860/4250	Curtis et al. 1999
32	NE Canada	GSD	7980/3250/6380	Barber et al. 2002
33	W Antarctic	Inclination	7560/3090	Brachfeld et al. 2000
34	Cariaco Basin	GSD	7180	Haug et al. 2001
35	Cariaco Basin	Titanium	none	Haug et al. 2001
36	Cariaco Basin	SST	8750	Lea et al. 2003
37	Bermuda Rise	δ^{18}O	8830/3950	Keigwin 1996
38	Botuvera Cv, Brasil	δ^{18}O	7920	Cruz Jr et al. 2005
39	Greenland Ice	Be^{10}	9150/4460/4260	Finkel and Nishiizumi 1997
40	Greenland Ice	δ^{18}O	8740/7110	Grootes and Stuiver 1997
41	Greenland Ice	SSN	8320	Solanki et al. 2004
42	Greenland Ice	δ^{14}C	none	Stuiver et al. 1998
43	W Atlantic	δ^{18}O (Tu)	7800/4760	Arz and Gerhardt 2001
44	W Atlantic	δ^{18}O	9450/6180/5220	Arz and Gerhardt 2001
45	Eq Atlantic	ΔSST	none	Kim and Schneider 2003
46	N Atlantic	HSG	3830	Gupta et al. 2003
47	N Atlantic	LG	4750	Bond 1997
48	Trop Atlantic	δ^{18}O	6550	Knaack 1997
49	Trop Atlantic	SST	none	DeMenocal et al. 2000
50	N Atlantic	HSG	4100	Bond et al. 2001
51	Canary	δ^{18}O	none	Freudenthal et al. 2002
52	Ireland	δ^{18}O	8960/8140	McDermott 2004
53	NW Morocco	δ^{18}O	7850/3930/4080	Hodell et al. 2001a
54	SW Europe	ΔT	8970/3320	Davis et al. 2003
55	NW Europe	ΔT	none	Davis et al. 2003
56	S Atlantic	LG	8760/3820/3190	Hodell et al. 2001b
57	Swiss Alpes	T7	7950/6030	Wick et al. 2003
58	Swiss Alpes	P	7920	Wick et al. 2003
59	Swiss Alpes	P	7920/5980	Wick et al. 2003
60	C Italy	Mg/Ca T	5950/3270	Drysdale et al. 2006
61	Angola Basin	U^k_{37}SST	none	Kim and Schneider 2003
62	C Italy	δ^{18}O	5950	Drysdale et al. 2006
63	S Germany	δ^{18}O	8130/8050/7190	von Grafenstein et al. 1998
64	Sahel	δ^{18}O	9070/6190	Gasse 2002
65	N Atlantic	SST	7430/4820	Sarnthein et al. 2003
66	N Norway	T	6940	Husum and Hald 2004
67	Sweden	GSD	9180/8350 7700/3760	Rubensdotter and Rosqvist 2003
68	N Finland	T	6940/5160	Husum and Hald 2004
69	N Atlantic	GSD	9380/9300 8090/3790	Chapman and Shackleton 2000
70	Marmara Sea	δ^{18}O	3590/3230	Sperling et al. 2003
71	Marmara Sea	U^k_{37} SST	7640/7250/3500	Sperling et al. 2003
72	SE Africa	δ^{18}O	9100	Holmgren et al. 2003
73	Burundi	P	9500/7320	Bonnefille and Chalié 2000
74	Black Sea	Ti	7220	Bahr et al. 2005
75	SE Europe	ΔT	8370/7820	Davis et al. 2003
76	Kola	δ^{18}O	8180/3550	Jones et al. 2004
77	Lk Victoria	Diatoms	9150/8350/7740 7370/7290	Stager et al. 2003
78	Lk Malawi	Si	9300	Johnson et al. 2002
79	Lk Malawi	MAR	none	Johnson et al. 2002
81	Soreq Cv, Israel	δ^{18}O	7170/4450	Bar-Matthews et al. 1999
82	Red Sea	δ^{18}O	9090/3730	Seeberg-Elverfeldt et al. 2004
83	Lk Sim, Kenia	δ^{18}O	8530/5590/4980	Barker et al. 2001
84	Lk Hall, Kenia	δ^{18}O	5250/4730	Barker et al. 2001
85	Kilimanjaro	δ^{18}O	4110	Thompson et al. 2002
86	Lk Abhe, Ethiopia	Level	8870/6800	Gasse 2000
87	Somalia	δ^{18}O	8890/8100 7340/6900	Jung et al. 2004
88	Qunf Cv, Oman	δ^{18}O	none	Fleitmann et al. 2007
89	Oman	δ^{18}O	6940/5220/4370	Fleitmann et al. 2003
90	Arabian Sea	δ^{18}O	8970/7730	Gupta et al. 2003
91	Arabian Sea	SSTW	none	Schulz 1995
92	NE Arabian Sea	δ^{18}O	none	Doose-Rolinski et al. 2001
93	NW Siberia	T7	none	Hantemirov and Shiyatov 2002
94	E Arabian Sea	δ^{18}O	8740/4720	Sarkar et al. 2000
95	Lk Issyk-Kul, Kyrgyzstan	δ^{18}O	8360/7950/7670	Ricketts et al. 2001
96	Tibet	δ^{18}O	none	Fontes et al. 1996
97	Dunde, China	δ^{18}O	7500/6970/6810 6260/5770	Jung et al. 2004
98	Komsomolskaia	δ^{2}H	6860/6460	Masson 2000
99	N Siberia	Pollen	3490	Andreev et al. 2003
100	NW China	P (AC)	8050	Herzschuh et al. 2004
101	NW China	P (Ef)	7460/6210	Herzschuh et al. 2004
102	Dongge Cv, China	δ^{18}O	7830/5190	Wang et al. 2005
103	Vostok, Antarctica	δ^{2}H	7080	Petit et al. 1999
104	N China	Clay	8980/3760	Xiao et al. 2002
105	S China	Moisture	9240	Liu et al. 2000
106	Xiangshui Cv, China	δ^{18}O	4960	Zhang et al. 2004
107	S China Sea	δ^{18}O	9490	Kienast et al. 2001
108	N China	GSD	8990/3980/7350	Jin et al. 2004
109	S China Sea	δ^{18}O	8450	Wang et al. 1999
110	Taiwan	LOI	5200/3950	Huang et al. 1997
111	S China Sea	SSS	8340/7440/7260 7110/5750	Jung et al. 2004
112	S China Sea	δ^{18}O	8600/5380	Wang et al. 1999
113	S China Sea	Silt	4740/3320/3070	Wang et al. 1999
114	S China Sea	δ^{18}O	7630/7460/5930	Wang et al. 1999
115	Dongge Cv, China	δ^{18}O	none	Yuan et al. 2004
116	Sulu Sea	δ^{18}O	3240/7730	Rosenthal 2003
117	W Pacific	δ^{18}O (81)	none	Stott et al. 2004
118	E China Sea	SST	9370	Sun et al. 2005
119	E China Sea	SST	none	Fengming et al. 2008
120	W Pacific	δ^{18}O	none	Rosenthal 2003
121	W Pacific	δ^{18}O (76)	8420/7270	Stott et al. 2004
122	NW Pacific	%Nitzschia	6290/4880	Shimada et al. 2004
123	NW Pacific	%Ozeanica	6170	Shimada et al. 2004
124	S Australia	T	none	Cook and Buckley 2000
125	Tasmania	T	none	Cook and Buckley 2000
126	SW Australia	Particles	8410/8310	Stanley and Deckker 2002
127	Taylor dome	δ^{18}O	3750	Grootes et al. 2001
128	Taylor dome	δ^{2}H	none	Steig et al. 1998
129	Lk Ioannina, Greece	δ^{18}O	4050	Frogley and Griffiths 2001
131	Lk Akgöl, Turkey	δ^{18}O	none	Roberts et al. 2008
132	Lk Acigöl, Turkey	δ^{18}O	3160	Roberts et al. 2011
133	Lk Frassino, Italy	δ^{18}O	none	Roberts et al. 2008
134	Lk Gölhisar, Turkey	δ^{18}O	3070	Roberts et al. 2011
135	Lk Pergusa, Italy	δ^{18}O	6620	Roberts et al. 2008

References

Abbott, M. B., Binford, M. W., Brenner, M., Curtis, J. H., Kelts, K. R., 1997. A 3,500 14C yr high-resolution sediment record of lake level changes in Lake Titicaca, Bolivia/Peru. Quaternary Research 47 (2), 169–180.

Andreev, A. A., Tarasov, P. E., Siegert, C., Ebel, T., Klimanov, V. A., Melles, M., Bobrov, A. A., Dereviagin, A. Y., Lubinski, D. J., Hubberten, H.-W., Sep. 2003. Late Pleistocene and Holocene vegetation and climate on the northern Taymyr Peninsula, Arctic Russia. Boreas 32 (3), 484–505.

Arz, H. W., Gerhardt, S., 2001. Millennial-scale changes of surface- and deep-water flow in the western tropical Atlantic linked to Northern Hemisphere high-latitude climate during the Holocene. Geology 29 (3), 239–242.

Bahr, A., Lamy, F., Arz, H. W., Kuhlmann, H., Wefer, G., Feb. 2005. Late glacial to Holocene climate and sedimentation history in the NW Black Sea. Marine Geology 214 (4), 309–322.

Bar-Matthews, M., Ayalon, A., Kaufman, A., Wasserburg, G. J., 1999. The Eastern Mediterranean paleoclimate as a reflection of regional events: Soreq cave, Israel. Earth and Planetary Science Letters 166 (1-2), 85–95.

Barber, D. C., Dyke, A., Hilaire-Marcel, C., Jennings, A. E., Andrews, J. T., Kerwin, M. W., Bilodeau, G., McNeely, R., Soutn, J., Morehead, M. D., Gagnon, J.-M., 2002. Forcing of the cold event of 8,200 years ago by catastrophic drainage of Laurentide lakes. Nature 400 (6742), 344–348.

Barker, P. A., Street-Perrott, F. A., Leng, M. J., Greenwood, P. B., Swain, D. L., Perrott, R. A., Telford, R. J., Ficken, K. J., 2001. A 14,000-Year Oxygen Isotope Record from Diatom Silica in Two Alpine Lakes on Mt. Kenya. Science 292 (5525), 2307–2310.

Begon, M., Harper, J. L., Townsend, C. R., 1993. Ecology—Individual, Populations and Communities, 2nd Edition. Blackwell Scientific Publications, Oxford.

Benson, L., Kashgarian, M., Rye, R., Lund, S., Paillet, F., Smoot, J., Kester, C., Mensing, S., Meko, D., 2002. Holocene multidecadal and multicentennial droughts affecting Northern California and Nevada. Quaternary Science Reviews 21 (4-6), 659–682.

Bloom, D. E., Sachs, J. D., Collier, P., Udry, C., 1998. Geography, demography and economic growth in {A}frica. Brookings Papers on Economic Activity 1998 (2), 207–295.

Bond, G., Nov. 1997. A Pervasive Millennial-Scale Cycle in North Atlantic Holocene and Glacial Climates. Science 278 (5341), 1257–1266.

Bond, G., Kromer, B., Beer, J., 2001. Persistent solar influence on North Atlantic climate during the Holocene. Science 294 (5549), 2130–2136.

Bonnefille, R., Chalié, F., 2000. Pollen-inferred precipitation time-series from equatorial mountains, Africa, the last 40 kyr BP. Global and Planetary Change 26 (1-3), 25–50.

Brachfeld, S., Acton, G. D., Guyodo, Y., Banerjee, S. K., Sep. 2000. High-resolution paleomagnetic records from Holocene sediments from the Palmer Deep, Western Antartic Peninsula. Earth and Planetary Science Letters 181 (3), 429–441.

Braidwood, L., Braidwood, R. J., 1949. On the treatment of the prehistoric Near Eastern materials in Steward's "Cultural Causality and Law". American Anthropologist 51 (4), 665–669.

Camill, P., Umbanhowar Jr, C. E., Teed, R., Geiss, C. E., Aldinger, J., Dvorak, L., Kenning, J., Limmer, J., Walkup, K., 2003. Late-glacial and Holocene climatic effects on fire and vegetation dynamics at the prairie forest ecotone in south-central Minnesota. Journal of Ecology 91 (5), 822– 836.

Carcaillet, C., Bergeron, Y., Richard, P. J. H., Fréchette, B., Gauthier, S., Prairie, Y. T., 2001. Change of fire frequency in the eastern Canadian boreal forests during the Holocene: does vegetation composition or climate trigger the fire regime ? Journal of Ecology 89 (6), 930 – 946.

Chapman, M., Shackleton, N., May 2000. Evidence of 550-year and 1000-year cyclicities in North Atlantic circulation patterns during the Holocene. The Holocene 10 (3), 287–291.

Claussen, M., Brovkin, V., 1999. A new model for climate system analysis: Outline of the model and application to palaeoclimate simulations. Environmental Modeling and Assessment 4 (4), 209–216.

Cook, E., Buckley, B., 2000. Warm-season temperatures since 1600 BC reconstructed from Tasmanian tree rings and their relationship to large-scale sea surface temperature anomalies. Climate Dynamics 16 (2-3), 79–91.

Cruz Jr, F. W., Burns, S. J., Karmann, I., Sharp, W. D., Vuille, M., Cardoso, A. O., Ferrari, J. A., Dias, P. L. S., Viana Jr., O., 2005. Insolation-driven changes in atmospheric circulation over the past 116,000 years in subtropical Brazil. Nature 434 (7029), 63–66.

Curtis, J. H., Brenner, M., Hodell, D. A., 1999. Climate change in the Lake Valencia Basin, Venezuela, \approx 12600 yr BP to present. The Holocene 9 (5), 609–619.

Curtis, J. H., Brenner, M., Hodell, D. A., Balser, R. A., Islebe, G. A., Hooghiemstra, H., 1998. A multi-proxy study of Holocene environmental change in Lowlands of Peten, Guatemala. Journal of Paleolimnology 19 (2), 139–159.

Davis, B. A. S., Brewer, S., Stevenson, A. C., Guiot, J., Jul. 2003. The temperature of Europe during the Holocene reconstructed from pollen data. Quaternary Science Reviews 22 (15-17), 1701–1716.

Davis, O. K., 1992. Rapid Climate Change in Coastal Southern California Inferred from Pollen analysis of San Joaquin Marsh. Quaternary Research 23 (1), 227–235.

DeMenocal, P. B., Ortiz, J., Guilderson, T., Adkins, J., Sarnthein, M., Baker, L., Yarusinsky, M., 2000. Abrupt onset and termination of the African Humid Period: rapid climate responses to gradual insolation forcing. Quaternary science reviews 19 (1-5), 347–361.

Denniston, R. F., Gonzalez, L. A., Baker, R. G., Reagan, M. K., Asmerom, Y., Edwards, R. L., Alexander, E. C., Nov. 1999. Speleothem evidence for Holocene fluctuations of the prairie-forest ecotone, north-central USA. The Holocene 9 (6), 671–676.

Doose-Rolinski, H., Rogalla, U., Scheeder, G., 2001. High resolution temperature and evaporation changes during the late Holocene in the northeastern Arabian Sea. Paleoceanography 16 (4), 358–367.

Dorale, J. A., Gonzalez, L. A., Reagan, M. K., Pickett, D. A., Murrell, M. T., Baker, R. G., 1992. A High-Resolution Record of Holocene Climate Change in Speleothem Calcite from Cold Water Cave, Northeast Iowa. Science 258 (5088), 1626–1630.

Drysdale, R., Zanchetta, G., Hellstrom, J., Maas, R., Fallick, A., Pickett, M., Cartwright, I., Piccini, L., 2006. Late Holocene drought responsible for the collapse of Old World civilizations is recorded in an Italian cave flowstone. Geology 34 (2), 101–104.

Ehrlich, P. R., Holdren, J. P., Mar. 1971. Impact of population growth. Science 171 (977), 1212–1217.

Fengming, C., Tiegang, L., Lihua, Z., Jun, Y., 2008. A Holocene paleotemperaturerecordbased on radiolaria from the northern Okinawa Trough (East China Sea). Quaternary International 183 (1), 115–122.

Finkel, R. C., Nishiizumi, K., 1997. Beryllium 10 concentrations in the Greenland Ice Sheet Project 2 ice core from 340 ka. Journal of Geophysical Research 102 (C12), 26699–26706.

Fisher, R. A., 1930. The Genetical Theory of Natural Selection. Dover, New York.

Fleitmann, D., Burns, S. J., Mangini, A., Mudelsee, M., Kramers, J., Villa, I., Neff, U., Al-Subbary, A. A., Buettner, A., Hippler, D., Matter, A., Sj, B., Aa, A.-s., Jan. 2007. Holocene ITCZ and Indian monsoon dynamics recorded in stalagmites from Oman and Yemen (Socotra). Quaternary Science Reviews 26 (1-2), 170–188.

Fleitmann, D., Burns, S. J., Mudelsee, M., Neff, U., Kramers, J., Mangini, A., Matter, A., 2003. Holocene Forcing of the Indian Monsoon Recorded in a Stalagmite from Southern Oman. Science 300 (5626), 1737–1739.

Fontes, J.-C., Gasse, F., Gibert, E., 1996. Holocene environmental changes in Lake Bangong basin (Western Tibet). Part 1: Chronology and stable isotopes of carbonates of a Holocene lacustrine core. Palaeogeography, Palaeoclimatology, Palaeoecology 120 (1-2), 25–47.

Freudenthal, T., Meggers, H., Henderiks, J., 2002. Upwelling intensity and filament activity off Morocco during the last 250,000 years. Deep Sea Research Part II: Topical Studies in Oceanography 49 (17), 3655–3674.

Frogley, M., Griffiths, H., 2001. Historical biogeography and Late Quaternary environmental change of Lake Pamvotis, Ioannina (northwestern Greece): evidence from ostracods. Journal of Biogeography 28 (6), 745–756.

Gallup, J. L., Sachs, J. D., 2000. Agriculture , Climate , and Technology: Why Are the Tropics Falling Behind ? American Journal of Agricultural Economics 82, 731–737.

Gasse, F., 2000. Hydrological changes in the African tropics since the Last Glacial Maximium. Quaternary Science Reviews 19 (1), 189–211.

Gasse, F., 2002. Diatom-inferred salinity and carbonate oxygen isotopes in Holocene waterbodies of the western Sahara and Sahel (Africa). Quaternary science reviews 21 (7), 737–767.

Gaston, K. J., 2000. Global patterns in biodiversity. Nature 405 (6783), 220–227.

Grootes, P. M., Steig, E. J., Stuiver, M., Waddington, E. D., Morse, D. L., Land, S. V., 2001. The Taylor Dome Antarctic 18 O Record and Globally Synchronous Changes in Climate 1. Quaternary Research 298 (3), 289–298.

Grootes, P. M., Stuiver, M., 1997. Oxygen 18/16 variability in Greenland snow and ice with 10ˆ{-3}- to 10ˆ5-year time resolution. Journal of Geophysical Research 102 (C12), 26455–26470.

Gupta, A. K., Anderson, D. M., Overpeck, J. T., 2003. Abrupt changes in the Asian southwest monsoon during the Holocene and their links to the North Atlantic Ocean. Nature 421 (6921), 4–7.

Hantemirov, R. M., Shiyatov, S. G., 2002. A continuous multimillennial ring-width chronology in Yamal, northwestern Siberia. The Holocene 12 (6), 717–726.

Haug, G. H., Hughen, K. A., Sigman, D. M., Peterson, L. C., Röhl, U., Aug. 2001. Southward migration of the intertropical convergence zone through the Holocene. Science 293 (5533), 1304–1308.

Herzschuh, U., Tarasov, P. E., Wu, B., Hartmann, K., 2004. Holocene vegetation and climate of the Alashan Plateau, NW China, reconstructed from pollen data. Palaeogeography, Palaeoclimatology, Palaeoecology 211 (1-2), 1 – 17.

Higuera-Gundy, A., Brenner, M., Hodell, D. A., Curtis, J. H., Leyden, B. W., Binford, M. W., Florida, I., 1999. A 10,300 14C yr Record of Climate and Vegetation Change from Haiti. Quaternary Research 170 (2), 159 –170.

Hodell, D. A., Curtis, J. H., Brenner, M., 1995. Possible role of climate in the collapse of the {C}lassic {M}aya Civilization. Nature 375 (6530), 391–394.

Hodell, D. A., Curtis, J. H., Sierro, F. J., Raymo, M. E., 2001a. Correlation of late Miocene to early Pliocene sequences between the Mediterranean and North Atlantic. Paleoceanography 16 (2), 164–178.

Hodell, D. A., Kanfoush, S., Shemesh, A., Crosta, X., 2001b. Abrupt cooling of Antarctic surface waters and sea ice expansion in the South Atlantic sector of the Southern Ocean at 5000 cal yr BP. Quaternary International 198 (2), 191–198.

Holmgren, K., Lee-Thorp, J. a., Cooper, G. R., Lundblad, K., Partridge, T. C., Scott, L., Sithaldeen, R., Siep Talma, A., Tyson, P. D., Nov. 2003. Persistent millennial-scale climatic variability over the past 25,000 years in Southern Africa. Quaternary Science Reviews 22 (21-22), 2311–2326.

Hu, F. S., Ito, E., Brubaker, L. B., Anderson, P. M., 1998. Ostracode Geochemical Record of Holocene Climatic Change and Implications for Vegetational Response in the Northwestern Alaska Range. Quaternary Research 95 (49), 86–95.

Huang, C., Liew, P., Zhao, M., 1997. Deep sea and lake records of the Southeast Asian paleomonsoons for the last 25 thousand years. Earth and Planetary . . . 146 (1-2), 59–72.

Hughes, M. K., Graumlich, L. J., 1996. Climatic variations and forcing mechanisms of the last 2000 years. Multi-millenial dendroclimatic studies from the western {U}nited {S}tates. NATO ASI Series Global Environmental Change 41, 109–124.

Husum, K., Hald, M., Nov. 2004. A continuous marine record 80001600 cal. yr BP from the Malangenfjord, north Norway: foraminiferal and isotopic evidence. The Holocene 14 (6), 877–887.

Jin, Z., Wu, J., Cao, J., Wang, S., Shen, J., Sep. 2004. Holocene chemical weathering and climatic oscillations in north China: evidence from lacustrine sediments. Boreas 33 (3), 260–266.

Johnson, T. C., Brown, E. T., Mcmanus, J., Barry, S., 2002. A High-Resolution Paleoclimate Record Spanning the Past 25,000 Years in Southern East Africa. Science 296 (5565), 3–6.

Jones, V., Leng, M. J., Solovieva, N., Sloane, H., Tarasov, P. E., 2004. Holocene climate of the Kola Peninsula; evidence from the oxygen isotope record of diatom silica. Quaternary Science Reviews 23 (7-8), 833–839.

Jung, S. J. A., Davies, G. R., Ganssen, G. M., Kroon, D., 2004. Synchronous {H}olocene sea surface temperature and rainfall variations in the {A}sian monsoon system. Quaternary Science Reviews 23 (20-22), 2207–2218.

Keigwin, L. D., 1996. The little {I}ce {A}ge and medieval warm period in the {S}argasso {S}ea. Science 274 (5292), 1503–1508.

Kienast, M., Calvert, S. E., Pelejero, C., Grimalt, J. O., 2001. A critical review of marine sedimentary \partialˆ{13}C org–p{CO}_2 estimates: New palaeorecords from the {S}outh {C}hina {S}ea and a revisit of other low-latitude \partialˆ{13}C org–p{CO}_2 records. Global Biogeochemical Cycles 15 (1), 113–127.

Kim, J.-H., Schneider, R. R., Sep. 2003. Low-latitude control of interhemispheric sea-surface temperature contrast in the tropical Atlantic over the past 21 kyears: the possible role of SE trade winds. Climate Dynamics 21 (3-4), 337–347.

Kisdi, E., Geritz, S. A. H., Jul. 2010. Adaptive dynamics: a framework to model evolution in the ecological theatre. Journal of Mathematical Biology 61 (1), 165–9.

Knaack, J. J., 1997. Eine neue {T}ransferfunktion zur {R}ekonstruktion der {P}aläoproduktivität aus {G}emeinschaften mariner {D}iatomeen. Berichte des Geologisch-Paläontologischen Instituts der Universität zu Kiel 83, 1–118.

Lachniet, M. S., Asmerom, Y., Burns, S. J., Patterson, W. P., Polyak, V. J., Seltzer, G. O., 2004. Tropical response to the 8200 yr B.P. cold event? Speleothem isotopes indicate a weakened early Holocene monsoon in Costa Rica. Geology 32 (11), 957–960.

Laird, K. R., Fritz, S. C., Maasch, K. A., Cumming, B. F., 1996. Greater drought intensity and frequency before {A.D.}˜1200 in the northern {G}reat {P}lains, {USA}. Nature 384 (6609), 552–554.

Lamy, F., Hebbeln, D., 2001. Holocene rainfall variability in southern Chile: a marine record of latitudinal shifts of the Southern Westerlies. Earth and Planetary Science Letters 185 (3-4), 369–382.

Lamy, F., Ru, C., Hebbeln, D., Wefer, G., America, S., 2002. High- and low-latitude climate control on the position of the southern Peru-Chile Current during the Holocene. October 17 (1028), 10.

Lea, D. W., Pak, D. K., Peterson, L. C., Hughen, K. A., 2003. Synchroneity of tropical and high-latitude Atlantic temperatures over the last glacial termination. Science 301 (5638), 1361–1364.

Leemans, R., Cramer, W. P., Nov. 1991. The {IIASA} database for mean monthly values of temperature, precipitation and cloudiness of a global terrestrial grid. Research report, International Institute of Applied Systems Analyses, Laxenburg.

Lemmen, C., 2010. World distribution of land cover changes during Pre- and Protohistoric Times and estimation of induced carbon releases. Géomorphologie : relief, processus, environnement 4 (2009), 303–312.

Lemmen, C., Wirtz, K. W., 2010. Socio-technological revolutions and migration waves: re-examining early world history with a numerical model. In: Gronenborn, D., Petrasch, J. (Eds.), The Spread of the Neolithic to Central Europe. Vol. 4,1 of RGZM Tagungen. Verlag des Römisch-Germanischen Zentralmuseums, Mainz, pp. 25–38.

Lieth, H., 1975. Modeling the primary productivity of the world. Primary Productivity of the Biosphere 14, 237–263.

Liu, J., Houyuan, L., Negendank, J., Mingram, J., Xiangjun, L., Wenyuan, W., Guoqiang, C., 2000. Periodicity of {H}olocene climatic variations in the {H}uguangyan {M}aar {L}ake. Chinese Science Bulletin 45 (18), 1712–1718.

Masson, V., Nov. 2000. Holocene Climate Variability in Antarc-

tica Based on 11 Ice-Core Isotopic Records. Quaternary Research 54 (3), 348–358.
McDermott, F., 2004. Palaeo-climate reconstruction from stable isotope variations in speleothems : a review. Quaternary Science Reviews 23 (7-8), 901–918.
Moy, C. M., Seltzer, G. O., Rodbell, D. T., Anderson, D. M., 2002. Variability of {E}l {N}iño/{S}outhern {O}scillation activity at millennial timescales during the {H}olocene epoch. Nature 420 (6912), 162–165.
Noren, A. J., Bierman, P. R., Lini, A., 2002. Millennial-scale storminess variability in the northeastern United States during the Holocene epoch. Nature 419 (6909), 821–824.
Oba, T., Murayama, M., 2004. Sea-surface temperature and salinity changes in the northwest Pacific since the Last Glacial Maximum. Journal of Quaternary Science 19 (4), 335–346.
Petit, J. R., Raynaud, D., Basile, I., Chappellaz, J., Davisk, M., Ritz, C., Delmotte, M., Legrand, M., Lorius, C., Pe, L., Saltzmank, E., 1999. Climate and atmospheric history of the past 420,000 years from the Vostok ice core, Antarctica. Time 399 (6735), 429–436.
Renfrew, C., Level, E. V., 1979. Exploring dominance: predicting polities from centers. In: Renfrew, C., Cooke, K. (Eds.), Transformations: Mathematical Approaches to Culture Change. Academic Press, New York, pp. 145–166.
Ricketts, R. D., Johnson, T. C., Brown, E. T., Rasmussen, K. A., Romanovsky, V. V., 2001. The Holocene paleolimnology of Lake Issyk-Kul, Kyrgyzstan: trace element and stable isotope composition of ostracodes. Palaeogeography, Palaeoclimatology, Palaeoecology 176 (1-4), 207–227.
Roberts, N., Eastwood, W. J., Kuzucuoglu, C., Fiorentino, G., Caracuta, V., Jan. 2011. Climatic, vegetation and cultural change in the eastern Mediterranean during the mid-Holocene environmental transition. The Holocene 21 (1), 147–162.
Roberts, N., Jones, M., Benkaddour, A., Eastwood, W. J., Filippi, M., Frogley, M., Lamb, H., Leng, M. J., Reed, J., Stein, M., Stevens, L., Valero-Garcés, B., Zanchetta, G., Dec. 2008. Stable isotope records of Late Quaternary climate and hydrology from Mediterranean lakes: the ISOMED synthesis. Quaternary Science Reviews 27 (25-26), 2426–2441.
Rodbell, D. T., Seltzer, G. O., Anderson, D. M., Abbott, M. B., Enfield, D. B., Newman, J. H., 1999. An ˜15,000-Year Record of {E}l-{N}i{ñ}o Alluviation in Southwestern {E}cuador. Science 283 (5401), 516–520.
Rosenthal, Y., 2003. The amplitude and phasing of climate change during the last deglaciation in the Sulu Sea, western equatorial Pacific. Geophysical Research Letters 30 (8), 1–4.
Rubensdotter, L., Rosqvist, G., 2003. The effect of geomorphological setting on Holocene lake sediment variability, northern Swedish Lapland. Journal of Quaternary Science 18 (8), 757–767.
Sarkar, A., Ramesh, R., Somayajulu, B. L. K., Agnihotri, R., 2000. High resolution Holocene monsoon record from the eastern Arabian Sea. Earth and Planetary Science Letters 177 (3-4), 2000–2000.
Sarnthein, M., van Kreveld, S., Erlenkeuser, H., Grootes, P. M., Kucera, M., Pflaumann, U., Schulz, M., 2003. Centennial-to-millennial-scale periodicities of Holocene climate and sediment injections off the western Barents shelf, 75 N. Boreas 32 (3), 447–461.
Schulz, H., 1995. Meeresoberflächentemperaturen vor 10\:000 {J}ahren – {A}uswirkungen des frühholozänen {I}nsolationsmaximums. Berichte-reports, Geologisch-Paläontologischen Institut und Museum, Christian-Albrechts-Universität, Kiel.
Seeberg-Elverfeldt, I., Lange, C. B., Arz, H. W., Pätzold, J., Pike, J., Aug. 2004. The significance of diatoms in the formation of laminated sediments of the Shaban Deep, Northern Red Sea. Marine Geology 209 (1-4), 279–301.
Shimada, C., Ikehara, K., Tanimura, Y., Hasegawa, S., Sep. 2004. Millennial-scale variability of Holocene hydrography in the southwestern Okhotsk Sea: diatom evidence. The Holocene 14 (5), 641–650.
Solanki, S. K., Usoskin, I. G., Kromer, B., Schüssler, M., Beer, J., 2004. Unusual activity of the Sun during recent decades compared to the previous 11,000 years. Nature 431 (7012), 1084.
Sperling, M., Schmiedl, G., Emeis, K. C., Erlenkeuser, H., Grootes, P. M., 2003. Black Sea impact on the formation of eastern Mediterranean sapropel S1? Evidence from the Marmara Sea. Palaeogeography, Palaeoclimatology, Palaeoecology 190 (1), 9–21.
Stager, J. C., Cumming, B. F., Meeker, L. D., 2003. A 10,000-year high-resolution diatom record from Pilkington Bay, Lake Victoria, East Africa. Quaternary Research 59 (2), 172–181.
Stanley, S., Deckker, P. D., 2002. A Holocene record of allochthonous , aeolian mineral grains in an Australian alpine lake ; implications for the history of climate change in southeastern Australia. Journal of Paleolimnology 27 (2), 207–219.
Steig, E. J., Brook, E. J., White, J. W. C., Sucher, C. M., Bender, M. L., Lehman, S. J., Morse, D. L., Waddington, E. D., Clow, G. D., 1998. Synchronous Climate Changes in {A}ntarctica and the {N}orth {A}tlantic. Science 282 (5386), 92.
Stott, L. D., Cannariato, K. G., Thunell, R., Haug, G. H., Koutavas, A., Lund, S., 2004. Decline of surface temperature and salinity in the western tropical {P}acific {O}cean in the {H}olocene epoch. Nature 431 (7004), 56–59.
Stuiver, M., Reimer, P. J., Bard, E., Beck, J. W., Burr, G. S., Hughen, K. A., Kromer, B., McCormac, G., van der Plicht, J., Spurk, M., 1998. {INTCAL98} radiocarbon age calibration, 24,000–0\,cal\,{BP}. Radiocarbon 40 (3), 1041–1083.
Sun, D., Gagan, M. K., Cheng, H., Scott-Gagan, H., Dykoski, C. A., Edwards, R. L., Su, R., 2005. Seasonal and interannual variability of the Mid-Holocene East Asian monsoon in coral delta O-18 records from the South China Sea. Earth and planetary science letters 237 (1-2), 69–84.
Thompson, L. G., Mosley-thompson, E., Davis, M. E., Henderson, K. A., Brecher, H. H., Zagorodnov, V. S., Mashiotta, T. A., Lin, P.-n., Mikhalenko, V. N., Hardy, D. R., Beer, J., 2002. Kilimanjaro ice core records: Evidence of {H}olocene climate change in tropical {A}frica. Science 298 (5593), 589–593.
Thompson, L. G., Mosley-Thompson, E., Davis, M. E., Lin, P.-n., Henderson, K. A., Mashiotta, T. A., 2003. Tropical glacier and ice core evidence of climate change on annual to millennial time scales. Climatic Change 59 (1-2), 137–155.
von Grafenstein, U., Erlenkeuser, H., Müller, J., Jouzel, J., Johnsen, S. J., 1998. The cold event 8200 years ago documented in oxygen isotope records of precipitation in Europe and Greenland. Climate Dynamics 14 (2), 73–81.
Wang, L., Sarnthein, M., Erlenkeuser, H., 1999. East Asian monsoon climate during the Late Pleistocene: high-resolution sediment records from the South China Sea. Marine Geology 156 (1-4), 245–284.
Wang, Y., Cheng, H., Edwards, R., He, Y., 2005. The Holocene Asian monsoon: links to solar changes and North Atlantic climate. Science 308 (5723), 854–857.
Wang, Y., van Cappellen, P., 1996. A multicomponent reactive transport model of early diagenesis: Application to redox cycling in coastal marine sediments. Geochimica et Cosmochimica Acta 60 (16), 2993–3014.
Wick, L., Lemcke, G., Sturm, M., 2003. Evidence of Lateglacial and Holocene climatic change and human impact in eastern Anatolia: high-resolution pollen, charcoal, isotopic and geochemical records from the laminated sediments of Lake Van, Turkey. The Holocene 13 (5), 665–675.
Wirtz, K. W., Lemmen, C., 2003. A global dynamic model for the neolithic transition. Climatic Change 59 (3), 333–367.
Wirtz, K. W., Lohmann, G., Bernhardt, K., Lemmen, C., Dec. 2010. Mid-Holocene regional reorganization of climate variability: Analyses of proxy data in the frequency domain. Palaeogeography, Palaeoclimatology, Palaeoecology 298 (3-4), 189–200.
Xiao, J., Nakamura, T., Lu, H., Zhang, G., 2002. Holocene climate changes over the desert / loess transition of. Earth and Planetary Science Letters 197 (1-2), 11–18.
Yu, S.-y., 2003. Centennial-scale cycles in middle Holocene sea level along the southeastern Swedish Baltic coast. GSA Bulletin 115 (11), 1404–1409.

Yuan, D., Cheng, H., Edwards, R., 2004. Timing, duration, and transitions of the last interglacial Asian monsoon. Science 304 (5670), 575.

Zhang, M., Yuan, D., Lin, Y., Qin, J., 2004. A 6000-year high-resolution climatic record from a stalagmite in Xiangshui Cave, Guilin, China. The Holocene 14 (5), 697–702.